Robust Polar Amplification in Ice-Free Climates Relies on Ocean Heat Transport and Cloud Radiative Effects

MARK R. ENGLAND[a,b] AND NICOLE FELDL[b]

[a] *Department of Mathematics and Statistics, University of Exeter, Exeter, United Kingdom*
[b] *Department of Earth and Planetary Sciences, University of California, Santa Cruz, Santa Cruz, California*

(Manuscript received 15 March 2023, in final form 4 January 2024, accepted 12 January 2024)

ABSTRACT: A fundamental divide exists between previous studies that conclude that polar amplification does not occur without sea ice and studies that find that polar amplification is an inherent feature of the atmosphere independent of sea ice. We hypothesize that a representation of climatological ocean heat transport is key for simulating polar amplification in ice-free climates. To investigate this, we run a suite of targeted experiments in the slab ocean aquaplanet configuration of CESM2-CAM6 with different profiles of prescribed ocean heat transport, which are invariant under CO_2 quadrupling. In simulations without climatological ocean heat transport, polar amplification does not occur. In contrast, in simulations with climatological ocean heat transport, robust polar amplification occurs in all seasons. What is causing this dependence of polar amplification on ocean heat transport? Energy-balance model theory is incapable of explaining our results and in fact would predict that introducing ocean heat transport leads to less polar amplification. We instead demonstrate that shortwave cloud radiative feedbacks can explain the divergent polar climate responses simulated by CESM2-CAM6. Targeted cloud locking experiments in the zero ocean heat transport simulations are able to reproduce the polar amplification of the climatological ocean heat transport simulations, solely by prescribing high-latitude cloud radiative feedbacks. We conclude that polar amplification in ice-free climates is underpinned by ocean–atmosphere coupling, through a less negative high latitude shortwave cloud radiative feedback that facilitates enhanced polar warming. In addition to reconciling previous disparities, these results have important implications for interpreting past equable climates and climate projections under high-emissions scenarios.

SIGNIFICANCE STATEMENT: Polar amplification is a robust feature of climate change in the modern-day climate. However, previous climate modeling studies fundamentally do not agree on whether polar amplification occurs in ice-free climates. In this study, we find in a state-of-the-art climate model that, if ocean heat transport is neglected, the response to an increase in CO_2 is not polar amplified, whereas robust polar amplification occurs if ocean heat transport is included. Using targeted model experiments, we diagnose cloud radiative effects as the driver of this divergent behavior. We conclude that polar amplification is a robust feature of the atmosphere–ocean system. Our results have important implications for interpreting past warm climates and future projections under high-emissions scenarios.

KEYWORDS: Sea ice; Atmosphere-ocean interaction; Climate change; Climate models; Clouds; Idealized models

1. Introduction

Polar amplification, the phenomenon in which the polar regions experience an enhanced surface warming relative to the global average in response to an increase in radiative forcing, is a robust feature of the modern climate system as demonstrated by the observational record and comprehensive climate model simulations (e.g., Manabe and Wetherald 1975; Pithan and Mauritsen 2014; Davy et al. 2018; Previdi et al. 2021; England et al. 2021; Hahn et al. 2021). Previous studies have consistently shown that sea ice, and the atmospheric processes related to sea ice, are leading drivers of the magnitude and seasonality of polar amplification (Kumar et al. 2010; Screen and Simmonds 2010; Dai et al. 2019; Hahn et al. 2022). However, there is a lack of consensus as to whether robust polar amplification occurs in ice-free climates. Understanding whether polar amplification is a ubiquitous response inherent to the climate system, or instead is dependent on the presence of sea ice, has important implications for how we interpret climate change in past warm climates as well as projections of future climate change under high-emissions scenarios.

First, we note that we will broadly restrict the discussion to studies using the idealized aquaplanet configuration. This removes unnecessary complexity and allows for a cleaner comparison across different atmospheric models. The details and results of the relevant slab ocean aquaplanet-based modeling studies are summarized in Table 1. There are numerous differences between the experimental setup in each study, which makes direct comparison across the studies challenging, including in the representation of sea ice, configuration of insolation, and choice of climatological q-flux. The q-fluxes are added as adjustments to the surface energy balance of the

Denotes content that is immediately available upon publication as open access.

Supplemental information related to this paper is available at the Journals Online website: https://doi.org/10.1175/JCLI-D-23-0151.s1.

Corresponding author: Mark England, m.england2@exeter.ac.uk

DOI: 10.1175/JCLI-D-23-0151.1

TABLE 1. Slab ocean aquaplanet simulations used in previous modeling studies. We provide estimates of the polar amplification factor in response to either a doubling or quadrupling of CO_2 and other details of the individual experimental setups. When multiple global climate models were analyzed in each study, we report each individual value of the polar amplification factor. In boldface we highlight the five studies that are directly comparable because they are strictly based on ice-free slab ocean aquaplanet simulations with seasonally varying insolation.

Study	Polar amplification factor	Model	Insolation	Sea ice	Slab depth	q-flux	Notes
Russotto and Biasutti (2020)	**0.9, 1.0, 1.05, 1.2, 1.25, 1.3, 1.35, 1.35, 1.35, 1.45, 1.45, 1.5**	**12 TRACMIP models**	**Seasonal cycle**	**No**	**30 m**	**Annual mean**	
Kim et al. (2018)	**1.0**	**GFDL-AM2**	**Seasonal cycle**	**No**	**10 m**	**Zero**	
Shaw and Smith (2022)	**0.75**	**ECHAM6**	**Seasonal cycle**	**No**	**30–50 m**	**Zero**	**Slab ocean non-aquaplanet runs with nonzero q-flux have PA factor of 1.45**
Langen et al. (2012)	**1.5**	**CAM3**	**Seasonal cycle**	**No**	**50 m**	**Annual mean**	**Prescribed albedo**
Rencurrel and Rose (2018)	**>1**	**CAM4**	**Seasonal cycle**	**No**	**60 m**	**Zero**	**Prescribed albedo**
Langen and Alexeev (2007)	2.5	CCSM3	Annual average	No	50 m	Tuned	Prescribed albedo
Alexeev et al. (2005)	1.5, 2.0	GEOS, CCSM3	Annual average	No	50 m	Zero	Prescribed albedo
Feldl and Roe (2013)	3.0	GFDL-AM2	Perpetual equinox	Only albedo feedback	20 m	Zero	
Rose et al. (2014)	2.0, 3.0, 1.1	CAM3, GFDL-AM2, CAM4	Perpetual equinox	No	10 m	Zero	
Roe et al. (2015)	2.0	GFDL-AM2	Perpetual equinox	Yes, albedo feedback disabled	20 m	Zero	
Graversen et al. (2014)	1.6	CCSM4	Seasonal cycle	Yes, albedo feedback disabled	Variable	Seasonal cycle	Includes land
Ceppi and Hartmann (2016)	1.2	GFDL-AM2	Annual average	No	50 m	Zero	Cloud locking
Feldl et al. (2017)	1.0	GFDL-AM2	Seasonal cycle	Only albedo feedback	30 m	Zero	Ice albedo of 0.3 approximates ice-free climate
Park et al. (2018)	1.2	GFDL-AM2	Annual average	No	50 m	4 W m^{-2} global forcing	Forcing applied at surface rather than through CO_2

ocean mixed layer to account for the transport of heat by the ocean circulation in the slab ocean configuration. The majority of these aquaplanet-based studies conclude that polar amplification in response to an increase in radiative forcing is an inevitable feature of the climate system, with or without the presence of polar sea ice (Alexeev et al. 2005; Langen and Alexeev 2007; Langen et al. 2012; Feldl and Roe 2013; Rose et al. 2014; Roe et al. 2015; Park et al. 2018; Rencurrel and Rose 2018; Russotto and Biasutti 2020) with polar amplification factors approximately ranging from 1.25 to 2.0 according to the interquartile range of the ordered results from the individual climate models from these studies (Table 1). Here we define the polar amplification factor to be the surface temperature response poleward of 60° divided by the global surface temperature response, with values > 1 indicating polar amplification. The studies of Hall (2004) and Graversen et al. (2014) provide further support for this conclusion, although these are both based on simulations with realistic land configuration and a representation of sea ice with the albedo feedback disabled. In contrast, three studies (Feldl et al. 2017; Kim et al. 2018; Shaw and Smith 2022) show no polar amplification in ice-free aquaplanets, with a substantial polar damping found in the simulations of Shaw and Smith (2022).

Although the weight of modeling evidence seems to support the notion of polar amplification in ice-free climates, Kim et al. (2018) demonstrate that many of the studies that purport to find substantial polar amplification (Feldl and Roe 2013; Rose et al. 2014; Roe et al. 2015) may have overestimated the enhanced polar warming because of the methodological artifact of using perpetual equinox insolation conditions. Kim et al. (2018) also find that using annual-mean insolation (Langen and Alexeev 2007; Alexeev et al. 2005; Ceppi and Hartmann 2016; Park et al. 2018) moderately exaggerates the polar amplification compared to realistic seasonally varying insolation. It is also important to highlight that even with identical experimental setup, there can be substantial intermodel spread in the simulated ice-free polar amplification factor (Russotto and Biasutti 2020). As such, making robust conclusions from the existing literature is challenging.

To gain a deeper insight on this question, energy balance models are a valuable tool. Previous studies using a moist energy balance model have found polar amplification in simulations without sea ice cover due to changes in moist transport in response to an increase in radiative forcing (Merlis and Henry 2018; Feldl and Merlis 2021). Consistent with this, Södergren et al. (2018) and Beer and Eisenman (2022) find considerable polar amplification in energy balance models after disabling the ice albedo feedback, and hence removing the effects of sea ice loss. Taken together, evidence from the energy balance perspective suggests that a strong tendency for enhanced polar surface warming relative to the rest of the globe is pervasive in ice-free climates (Armour et al. 2019).

Which processes, independent of sea ice cover or sea ice loss, could contribute to polar amplification in general circulation models (GCMs)? One of the main potential drivers is changes in atmospheric heat transport. Previous studies using a range of model complexities (Flannery 1984; Alexeev et al. 2005; Cai 2005; Cai and Lu 2007; Henry et al. 2021) have reported that the transport of warm, moist air masses into the high latitudes can result in polar amplification. Most relevant for our purposes, this has been documented in a slab ocean aquaplanet which uses a novel technique for isolating the role of atmospheric transport (Graversen and Langen 2019). Evidence from other past climates also supports the importance of atmospheric transport (Rodgers et al. 2003). Some studies have cast doubt on the importance of changes in atmospheric transport in causing enhanced polar warming (Hwang et al. 2011; Kay et al. 2012) although these concerns are likely not relevant in ice-free climates because the sea ice albedo feedback is not present to minimize the role of transport (Alexeev and Jackson 2013). In addition, the water vapor feedback has been identified as a source of polar warming (Graversen and Wang 2009; Södergren et al. 2018; Russotto and Biasutti 2020; Henry et al. 2021). Despite the meridional structure peaking in the tropics, the water vapor feedback is associated with bottom heavy, surface amplified warming in the high latitudes (Henry et al. 2021). The last major factor that could contribute to polar amplification in ice-free climates is cloud feedbacks.

In the present-day climate, the role of cloud feedbacks in polar amplification is strongly tied to changes in sea ice cover (Vavrus et al. 2011a,b; Kay et al. 2016), with sea ice loss driving an increase in low cloud cover during autumn and winter and primarily influencing the surface climate through the longwave component (Holland and Bitz 2003; Taylor et al. 2013; Ceppi and Hartmann 2016). However, cloud feedbacks can be important independent drivers of polar amplification if the ice–albedo feedback is disabled (Graversen and Wang 2009; Södergren et al. 2018). In contrast to the present climate, global climate models simulate an overall decrease in cloudiness in response to increased radiative forcing in ice-free climates (Zhu et al. 2019) and the shortwave component of the cloud feedback becomes more important (Graversen and Wang 2009; Kim et al. 2018; Park et al. 2018). In addition, cloud microphysics can play a key role in shaping polar climate change (Tan and Storelvmo 2019; Tan et al. 2022). We can also gain perspective by looking to evidence from equable climates, warm episodes in the paleoclimate record such as the early Eocene (Huber and Caballero 2011) and early Cretaceous (Barron 1983), which had substantially warmer poles and diminished pole-to-equator temperature gradients. In these equable climates, changes in both low clouds (Cronin and Tziperman 2015; Zhu et al. 2019; Henry and Vallis 2022) and high clouds (Dutta et al. 2021, 2023) have potentially contributed to enhanced polar warming. In brief, cloud feedbacks play a complex but important role in polar amplification in today's climate and are likely to be more prominent, and different in nature, in ice-free climates.

Returning to the inconsistency in the existing modeling literature, if we strictly limit the comparison only to slab ocean aquaplanets with no representation of sea ice and with seasonally varying insolation, only five studies remain (bolded in Table 1). Three studies find polar amplification in ice-free climates (Langen et al. 2012; Rencurrel and Rose 2018; Russotto and Biasutti 2020) and two studies do not (Kim et al. 2018; Shaw and Smith 2022). However, there is a hint here in what is causing this lack of consensus in the literature: as can be

seen in Table 1, two studies that do simulate polar amplification prescribe a quasi-realistic climatological ocean heat transport (OHT) whereas the two studies that do not simulate polar amplification prescribe zero climatological OHT. We note that this divide is not perfect because the study of Rencurrel and Rose (2018), which prescribes a deeper mixed layer than the other studies, finds a modest polar amplification with zero OHT prescribed. OHT has been shown to influence many aspects of the climate system including the mean global temperature (Rencurrel and Rose 2018), the meridional temperature gradient (Rose and Ferreira 2013), climate sensitivity (Singh et al. 2022), tropical circulation changes (Chemke 2021), and polar amplification (Holland and Bitz 2003; Beer et al. 2020). In this study we will go on to demonstrate that the choice of climatological OHT is crucial for determining whether robust polar amplification occurs in ice-free climates.

2. Methods

a. *Aquaplanet setup*

We employ the state-of-the-art CMIP6-class atmospheric model of the Community Earth System Model version 2 (CESM2-CAM6) (Danabasoglu et al. 2020) in the aquaplanet configuration, a core component of the CESM project simple model initiative (Polvani et al. 2017). CESM2-CAM6 represents a substantial advance in atmospheric modeling capabilities compared to CESM1-CAM5, including the incorporation of a unified turbulence scheme, updates to the cloud microphysics scheme and an improved treatment of aerosols. As a result, the ability of CESM2-CAM6 to accurately simulate tropical precipitation, shortwave cloud forcing (Danabasoglu et al. 2020), many aspects of the large-scale circulation (Simpson et al. 2020), and the frequency of liquid containing Arctic clouds (McIlhattan et al. 2020) has substantially improved. The default version of CESM2-CAM6 has known deficiencies linked to its high climate sensitivity, such as its ability to simulate past climates. We run the CESM2-CAM6 in its Last Glacial Maximum climate constrained configuration (Zhu et al. 2022), which involves minor changes to the cloud microphysics and ice nucleation scheme and substantially lowers CESM2-CAM6's high climate sensitivity, in part from a reduction in shortwave cloud feedbacks and cloud aerosol interactions.

The atmospheric model CESM2-CAM6 is coupled to a slab ocean of 30 m mixed layer depth. For the purposes of this study, we do not include any representation of sea ice, allowing sea surface temperatures to drop below the freezing point. So as not to introduce any zonal or hemispheric asymmetries, the aerosol emissions and ozone concentrations, taken from the 1850 preindustrial control setup, are zonally averaged and symmetrized about the equator, while keeping the seasonal differences between the two hemispheres intact. Unlike many previous aquaplanet-based studies, our setup includes the full seasonal cycle (obliquity of 23.45° and eccentricity of 0). This is an important consideration because the results of Kim et al. (2018) demonstrate that the choice of insolation condition can lead to unphysical conclusions about the presence and magnitude of polar amplification.

We conduct pairs of simulations for each configuration of the OHT profiles described below: a $1xCO_2$ control simulation with a preindustrial CO_2 mixing ratio of 284.7 ppmv and a $4xCO_2$ perturbed simulation with a CO_2 mixing ratio of 1138.8 ppmv. All other forcings, including aerosol emissions and ozone concentrations, are identical in the $1xCO_2$ and $4xCO_2$ simulations. Each simulation is run for 120 years and the results we present are based on an average of the last 100 years, after each simulation has equilibrated. All simulations are run with a horizontal resolution of $1.9° \times 2.5°$ and 32 vertical levels. To check the robustness of the results in a different climate model, we repeat the core set of the simulations with CESM1-CAM5 aquaplanet (Medeiros et al. 2016). Despite belonging to the same model family, CESM1-CAM5 has a substantially different treatment of cloud microphysics and aerosols, as well as a lower equilibrium climate sensitivity (4.1°C) than the default configuration of CESM2-CAM6 (5.6°C) and is more in line with the ECS of the Last Glacial Maximum constrained version used in this study (4.1°C).

b. *q-fluxes*

Positive q-flux values indicate regions where the ocean is a local heat sink, and negative q-flux values indicate a local heat source, with the ocean transporting heat from the sink regions to the source regions. Care was taken during the process of idealizing the q-flux profiles to ensure that there is a global balance between heat entering and exiting the slab ocean so it does not act as an overall source or sink of heat. Last, it is important to emphasize that each $1xCO_2$ and $4xCO_2$ pair of simulations share the identical q-flux profile—we are not investigating how polar amplification responds to changes in OHT, rather how the climatological OHT controls the base climate and then in turn shapes the meridional structure of the response to an increase in radiative forcing.

1) ZERO OHT

Many previous studies (Kim et al. 2018; Shaw and Smith 2022; Alexeev et al. 2005; Feldl and Roe 2013; Rose et al. 2014; Roe et al. 2015) have made the simplification of neglecting climatological OHT by setting the q-flux to zero (Fig. 1a). We note here that the three slab ocean aquaplanet-based studies run with zero q-flux that are directly comparable to our simulations, because they feature seasonally varying insolation and do not include sea ice, simulate a range of responses: moderate polar amplification (Rencurrel and Rose 2018), no polar amplification (Kim et al. 2018), or polar-damped warming relative to the global mean (Shaw and Smith 2022).

2) 1850 ANNUAL-MEAN OHT

To include a representation of the modern climate's OHT, we calculate the annual-mean q-flux profile from 1000 years of the CESM2 1850 preindustrial control simulation (Fig. 1b). In the annual mean, the ocean transports heat from the tropics into the middle and high latitudes with a peak poleward OHT of 1.3 PW (Fig. S1b in the online supplemental material). This annual-mean q-flux profile is approximately consistent with that used in the study of Langen et al. (2012)

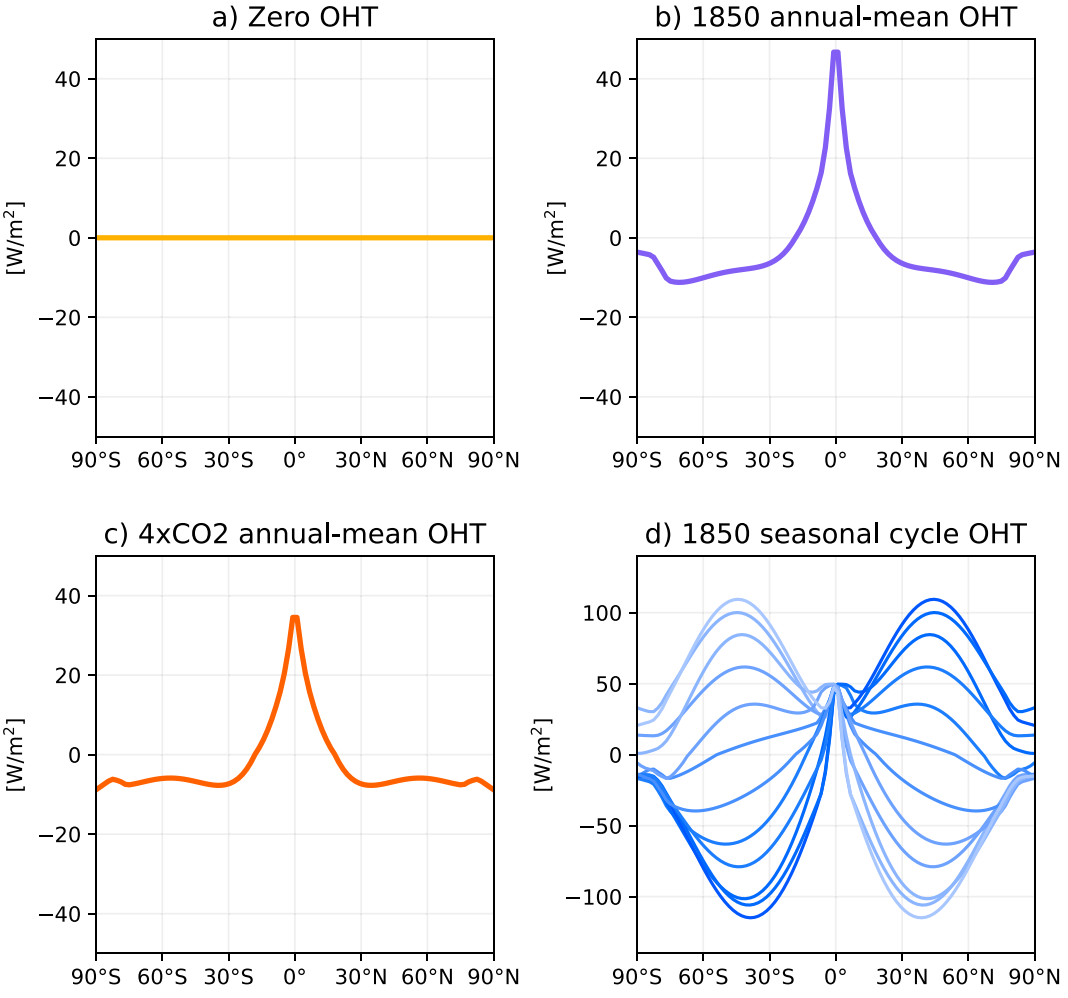

FIG. 1. Zonally uniform q-flux profiles (W m^{-2}) implemented in the CESM slab ocean aquaplanet simulations for the four different experimental configurations: (a) Zero OHT (yellow), (b) 1850 annual-mean OHT (purple), (c) 4xCO_2 annual-mean OHT (orange), and (d) 1850 seasonal cycle OHT. Positive values indicate heat flux from the atmosphere to the ocean (atmospheric heat sink) and negative values indicate heat flux from the ocean to the atmosphere (atmospheric heat source). Each profile integrated with respect to latitude results in a net of zero heat entering or exiting the atmosphere. In (d), the dark blue colors indicate the Northern Hemisphere cold months and the light blue colors indicate the Southern Hemisphere cold months. Note that (d) has a different vertical axis range than the other panels.

and in the multimodel study of Russotto and Biasutti (2020). These two studies, which again are based on simulations directly comparable to ours, largely show a polar-amplified response to increased radiative forcing in ice-free climates. We note that at the highest latitudes there is a decrease in the flux of heat from the ocean to the atmosphere which is due to two reasons: the presence of the Antarctic continent in the Southern Hemisphere and the multiyear sea ice covering the deep Arctic in the Northern Hemisphere.

3) 4xCO_2 ANNUAL MEAN OHT

It is possible that the presence of persistent sea ice cover in the preindustrial control q-flux profile could be inadvertently influencing our results pertaining to whether polar amplification is a robust phenomenon in ice-free climates. To remove any complicating trace of sea ice, we also include a representation of the climatological OHT in an ice-free climate by calculating the annual-mean q-flux profile from years 500 to 999 of the CESM2 4xCO_2 run (Fig. 1c). All sea ice cover has melted by the year 250 in the Northern Hemisphere and by the year 300 in the Southern Hemisphere (Bacmeister et al. 2020). As such, there is no possibility of the influence of sea ice being present in the 4xCO_2 q-flux profile. Compared to the 1850 annual-mean q-flux profile (Fig. 1b), the 4xCO_2 q-flux profile is qualitatively similar but has less export of heat from the tropics to the extratropics with a peak poleward heat transport of 1.1 PW (Fig. S1c). Last, and perhaps more importantly for our purposes, the 4xCO_2 q-flux profile has no ice-related reduction in the flux of heat from the ocean to the atmosphere at the highest latitudes. However, we note that

the role of the Antarctic landmass in reducing poleward heat transport at the highest latitude is still present and this could lead to a modest underestimation of the role of OHT on the high-latitude surface climate.

4) 1850 SEASONAL CYCLE OHT

It is important to consider whether the simplification of prescribing an annual-mean q-flux and removing the substantial seasonality of OHT, as has been done by previous studies (Russotto and Biasutti 2020; Langen et al. 2012), may influence the magnitude of simulated polar amplification. As such, we also perform an experiment based on the 1850 q-flux with a monthly-varying seasonal cycle (Fig. 1d). Comparing the annual-mean and seasonal cycle versions (Figs. 1b,d), it is clear that the seasonality of the ocean heat sink in the deep tropics is small, although the location of the peak flux from the atmosphere to the ocean does move off the equator seasonally. The largest differences are found in the midlatitudes where there is a huge seasonal swing from a maximum of over 100 W m^{-2} of heat entering the ocean in the warm season and a similar amount of heat leaving the ocean in the cold season. This seasonal range is extremely large, over 20 times the magnitude of the midlatitude annual-mean q-flux. Incorporating the seasonal cycle of OHT into our simulations introduces a seasonal storage of vast amounts of heat and results in an effective peak interhemispheric transport of nearly 20 PW (Fig. S1d).

c. *Cloud locking in CESM2*

To investigate the role of clouds in shaping the polar-amplified warming, we utilize a technique called "cloud locking" in new targeted sets of CESM2-CAM6 aquaplanet simulations. Cloud locking is a method that prescribes cloud radiative effects (CRE) over a certain region, with the rest of the climate system free to evolve. This approach has been scientifically validated in CESM2 and been used to study the effect of CRE on tropical climate (Medeiros et al. 2021; Benedict et al. 2020) and the extratropical storm tracks (Grise et al. 2019). Additionally, the same technique was implemented in CESM1 to investigate the role of Arctic CRE in driving Arctic surface warming (Middlemas et al. 2020).

Cloud locking in CESM2 involves prescribing the properties of clouds through 10 fields in the radiation code in the atmospheric model to a desired state, essentially prescribing cloud radiative heating rates. The climate can evolve and lead to changes in clouds, but instead of relying on predicted cloud fields, the prescribed cloud properties are employed to gauge the radiative effects on the atmospheric circulation. Conventionally, the fields are "locked" so that they cannot evolve in step with external forcing or internal climate variability and the climate evolution with CRE disabled can be isolated. Here, we take a somewhat different approach and prescribe the CRE from the 1850 annual-mean OHT simulations into the corresponding zero OHT simulations. In addition, we only perform the cloud locking poleward of 45°, which we shall broadly define as "higher-latitude clouds," with the CRE in the lower latitudes free to evolve. The choice of this latitude range was motivated to keep the meridional structure of the cloud field differences intact, which generally extended from the poles to the higher midlatitudes. Specifically, two cloud locking simulations are run: a 1xCO_2 zero OHT simulation with higher-latitude CRE prescribed from the 1xCO_2 1850 annual-mean OHT simulation and a 4xCO_2 zero OHT simulation with higher-latitude CRE prescribed from the 4xCO_2 1850 annual-mean OHT simulation. The difference between these two cloud locking simulations isolates the climate response to a quadrupling of CO_2 in the zero OHT climate if the zero OHT climate had the same higher-latitude CRE climatology and response as in the 1850 annual-mean OHT climate.

The cloud properties are prescribed in the cloud locking simulations at each 2-h step from 20 years of the 1850 annual mean OHT target experiments. This involves outputting 2-hourly cloud fields for 20 years in both of the 1850 annual mean OHT experiments. Despite being data intensive, 20 years was chosen to avoid interannual modes of internal climate variability from biasing the results. For every 2-h step, a year from the 20 years of cloud data is randomly selected and then the cloud properties are overwritten by the fields from the corresponding day and hour. The motivation for this is to eliminate autocorrelation in the prescribed cloud properties (Rädel et al. 2016). This process is explained in more detail in Grise et al. (2019), although we opted for the more comprehensive 20 years of target cloud data rather than three years. Please note that cloud locked simulations are only differenced with other cloud locked simulations. As for the main suite of experiments, both cloud locking simulations are run for 120 years and the results we present are based on an average of the last 100 years.

3. Results

We start by examining the meridional surface warming structure in response to a quadrupling of CO_2 in the CESM2 aquaplanet for the four different configurations of prescribed OHT (section 2b). The first key result is that polar amplification is present in the annual-mean surface temperature response in the simulations prescribed with 1850 annual-mean OHT, 4xCO_2 annual-mean OHT, and 1850 seasonal cycle OHT, but not in the zero OHT simulation (Fig. 2a). In fact, we find that the surface temperature response to a quadrupling of CO_2 in the zero OHT experiment is damped in the polar region (yellow line in Fig. 2a). We note that the magnitude of the annual-mean global-mean surface warming simulated by CESM2, consistent with the results of Rencurrel and Rose (2018), is also found to be dependent on the choice of climatological OHT (3.2 K for zero OHT, 5.6 K for 1850 annual-mean OHT, 5.0 for 4xCO_2 annual-mean OHT, and 6.0 for 1850 seasonal cycle OHT). After normalizing by the global-mean surface temperature response, the similarities and differences in the polar climate responses are even more evident (Fig. 2b). The three OHT experiments each simulate a polar amplification factor, defined as the ratio of the surface temperature response poleward of 60° to the global-mean value, of between 1.16 and 1.19 (16%–19% more warming in the polar regions as compared to the

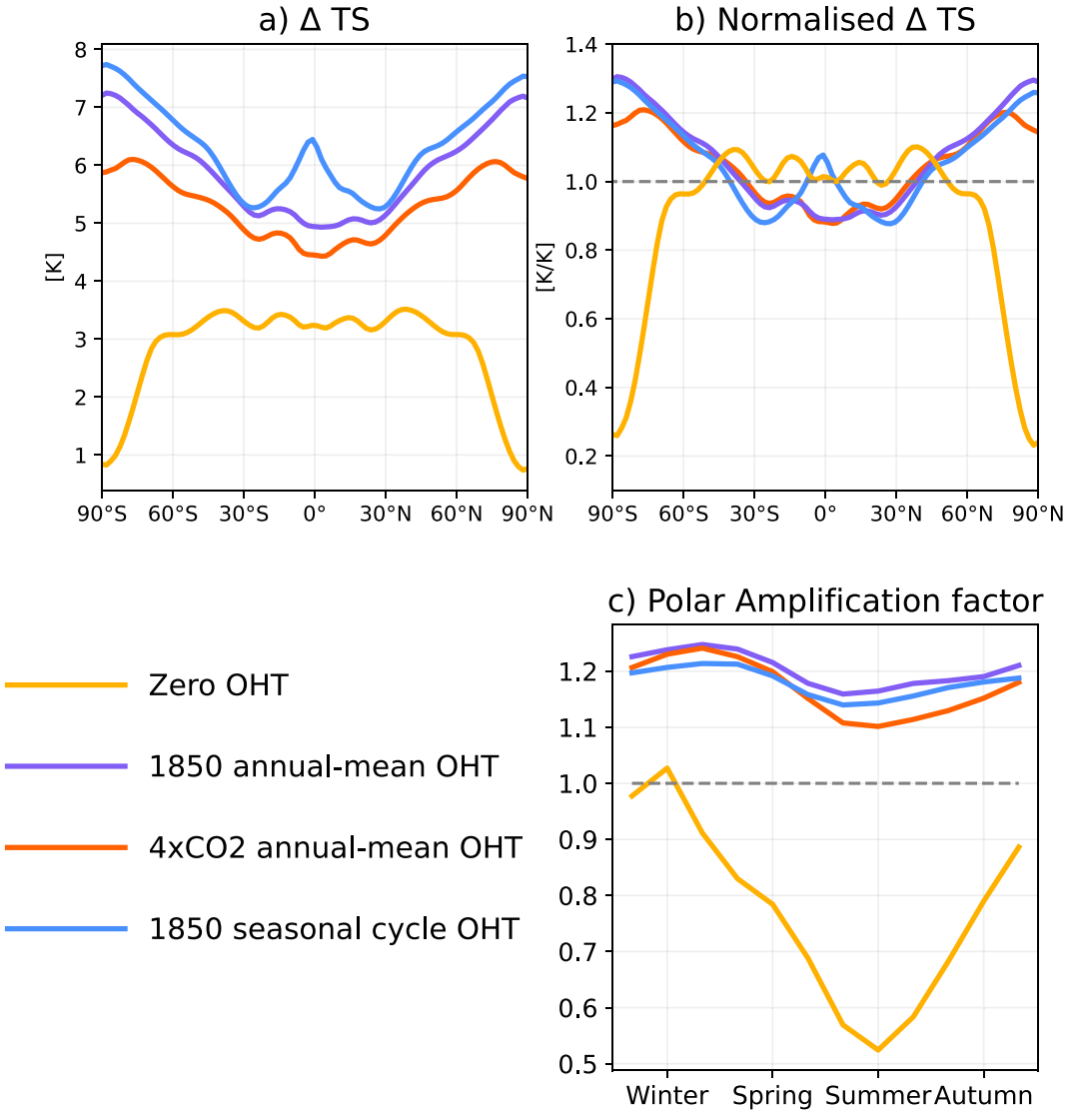

FIG. 2. (a) Zonal-mean annual-mean surface temperature response to a quadrupling of CO_2 for CESM2 aquaplanet experiments prescribed with zero OHT (yellow), 1850 annual-mean OHT (purple), 4xCO_2 annual-mean OHT (orange), and 1850 seasonal cycle OHT (blue). (b) As in (a), but the surface temperature response is normalized by its global-mean annual-mean value. (c) The monthly varying seasonal cycle of the polar amplification factor, defined as the surface warming poleward of 60° divided by the global-mean surface warming, in each set of simulations. The polar amplification factor is averaged over the polar regions of both hemispheres after aligning their seasonal cycle. In (b) and (c), the dashed gray line indicates the 1.0 line where the regional warming equals the global warming.

global mean) whereas the zero OHT experiment exhibits 24% less warming in the polar regions than the global-mean value, resulting in a polar amplification factor of 0.76. Remembering that each of these set of experiments is forced identically with a quadrupling of CO_2 with OHT unchanged under increasing CO_2, our results suggest that whether the response to an increase in radiative forcing is polar amplified is predetermined in this model by the inclusion, or lack thereof, of a quasi-realistic representation of climatological OHT. In the next section, we ask whether there is a simple mechanism, according to the diffusive perspective of atmospheric energy transport, that connects climatological OHT and enhanced polar amplification.

a. Moist EBM fails to capture polar amplification dependence on climatological ocean heat transport as simulated by GCMs

Can we gain insight from the moist EBM framework into why introducing a climatological poleward OHT leads to an enhanced surface warming in the polar regions relative to the lower latitudes in response to an increase in radiative forcing? We investigate this question by comparing the surface temperature

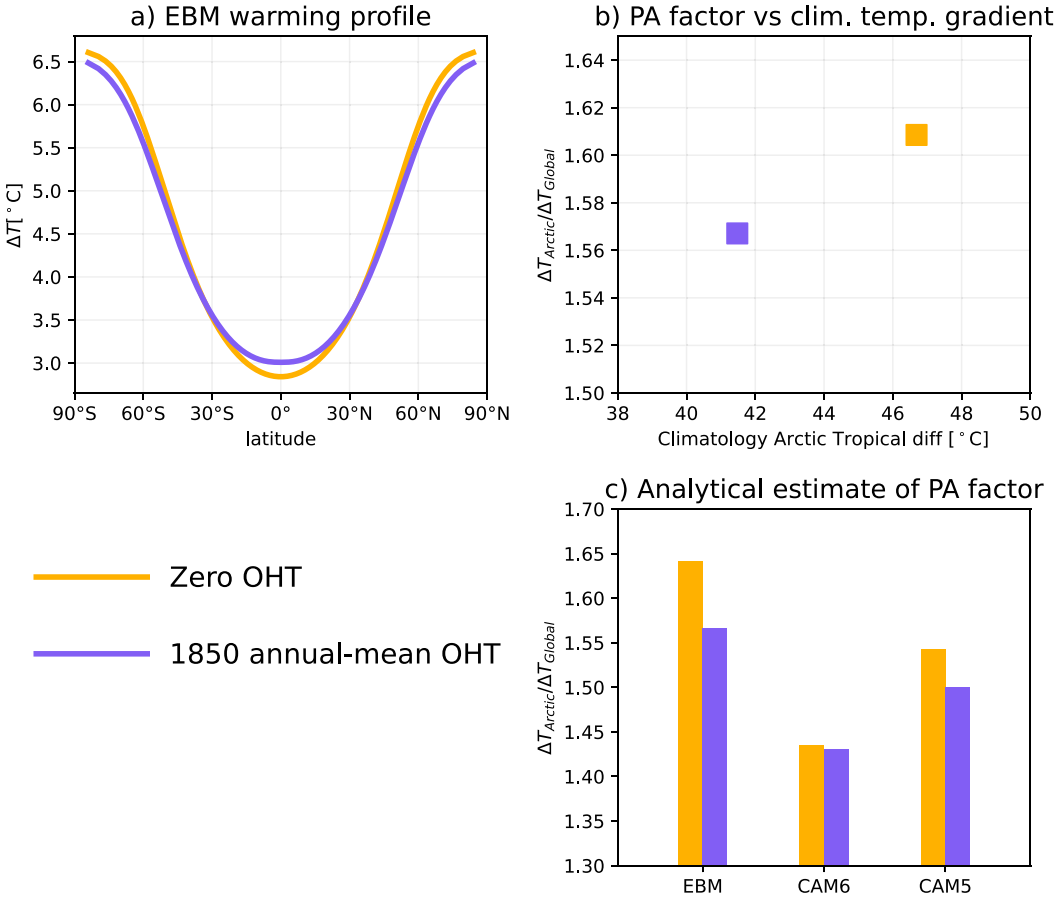

FIG. 3. (a) Meridional profile of annual-mean surface temperature response in the moist EBM to an increase in radiative forcing of 7.2 W m^{-2}. (b) Polar amplification factor of surface temperature response vs the annual-mean pole-to-equator temperature difference in the 1xCO_2 climate in the moist EBM. (c) Analytical approximation from Merlis and Henry (2018) of the polar amplification factor in the moist EBM, CESM2-CAM6, and CESM1-CAM5. In all panels, yellow indicates the zero OHT experiment and purple indicates the 1850 annual-mean OHT experiment.

response to a uniform 7.2 W m^{-2} increase in radiative forcing (approximately equivalent to a quadrupling of CO_2) as simulated by the moist EBM when prescribed with zero OHT and 1850 annual-mean OHT. The full details of the moist EBM setup are included in the appendix. Counter to the results from the GCM, we find that introducing a representation of OHT *reduces* the pole-to-equator gradient of the surface temperature response in the moist EBM (cf. the yellow and purple lines in Fig. 3a). What is driving this reduction in polar enhanced warming in the OHT climate relative to the zero OHT climate? A likely culprit is that the inclusion of OHT, by flattening meridional gradients in moist static energy, is accompanied by a compensating weakening in atmospheric energy transport in the 1xCO_2 climates. Indeed, in the annual mean, the climatological equator-to-pole surface temperature difference is larger in the zero OHT simulation than the 1850 annual-mean OHT simulation: 46.7 K compared to 41.5 K (Fig. 3b). In other words, introducing the climatological OHT reduced the pole-to-equator temperature difference by 5.2 K. As a consequence, the downgradient atmospheric transport of energy from the low to the high latitudes is larger in the zero OHT simulation, and it increases more under an increase in radiative forcing (not shown). Thus, the polar amplification factor is larger in the zero OHT experiment (1.61) than in the 1850 annual-mean OHT experiment (1.57) (Fig. 3b).

One difference that may explain the opposing behavior simulated by the GCM and the moist EBM is that the moist EBM starts from its own internally consistent 1xCO_2 climate, which will differ from the 1xCO_2 simulated by the GCMs. Specifically, the EBM has substantially colder high latitudes and so a much larger gradient in temperature from the equator to the poles. To test whether this is the source of the inconsistency, we turn to the analytical approximation of Merlis and Henry (2018), as briefly described in the appendix, to estimate the polar amplification factor the moist EBM would simulate given the 1xCO_2 climates from CESM2-CAM6 and CESM1-CAM5. As shown by Fig. 3c, according to the analytical approximation there is more polar-amplified warming in the zero OHT cases relative to the OHT cases whether the moist EBM, CESM2-CAM6, or CESM1-CAM5 1xCO_2 climates are used, although this difference is small in the case of CESM2-CAM6. The analytical estimate performs well at predicting the polar amplification factors for the moist EBM

(1.64 versus 1.61 for the zero OHT simulation and 1.57 versus 1.57 for the 1850 annual-mean OHT simulation) even though the analytical approximation is based on annual-mean insolation. Nevertheless, it is clearly evident that the analytical approximation based on moist EBM theory does not correctly predict that incorporating climatological OHT will lead to a robust increase in polar amplification in the GCM experiments.

What insights can be gained from this inconsistency between the EBM and the GCM experiments? First, this demonstrates that changes in atmospheric energy transport due to the alteration of the meridional energy gradient by OHT are not able to explain why the OHT GCM experiments are more polar amplified than their zero OHT counterparts. This raises the question about how applicable this diffusive perspective of atmospheric transport regarding polar amplification is in GCMs, and by extension the real world. Second, this suggests that there is some mechanism which is not included in the formulation of the moist EBM that not only correctly explains how climatological OHT influences polar amplification in the GCMs but also has to overcome the opposing effect of a weakened increase in atmospheric energy transport as anticipated by the EBM. In the rest of this study, we argue that this mechanism is through clouds and CRE.

b. *Occurrence of polar amplification in CESM2 aquaplanet predetermined by climatological ocean heat transport*

Returning to the CESM2-CAM6 simulations, we find a substantial difference in the seasonality of polar amplification between the OHT and zero OHT experiments. The OHT simulations all show a muted seasonal cycle with polar amplification throughout the year (Fig. 2c). We remind the reader that the amplitude of the seasonal cycle of polar amplification is much smaller here than in icy climates because sea ice–related processes are known to dominate the seasonality of enhanced polar warming (Hahn et al. 2022; Feldl and Merlis 2021). However, the results from our OHT simulations suggest a nonnegligible role for non-icy processes in shaping the timing of polar amplification because, as in icy climates, the polar-amplified warming response peaks in late winter (1.21–1.25) and has a minimum in the summer (1.10–1.16).

In contrast to the subdued seasonality of polar amplification found in the OHT experiments, the polar surface temperature response in the zero OHT experiment exhibits a pronounced seasonal dependence. The polar-damped response noted previously for this experiment arises from the summer months, when the polar regions exhibit nearly half as much warming as the global-mean response (Fig. 2c). We do not find appreciable polar amplification in the experiment with zero OHT in any month of the year. What is driving this strong seasonality without the presence of sea ice? The prominence of the summer polar damping indicates that shortwave feedbacks likely play an important role, consistent with the simulations of Graversen and Wang (2009). Hence, in the absence of sea ice as an explanatory factor, we propose that clouds are strongly mediating the differences in the high-latitude climate response between the OHT and zero OHT experiments.

Next, we return to two concerns raised in section 2b that motivated the inclusion of the $4xCO_2$ annual-mean OHT and 1850 seasonal cycle OHT simulations. First, *does the influence of sea ice cover on the 1850 annual-mean OHT at the high latitudes drive the polar-amplified warming response?* The answer here is a clear no; results from the 1850 annual-mean OHT simulations, which are derived from simulations featuring year-round sea ice, and the $4xCO_2$ annual-mean OHT simulations, which are derived from simulations that have no sea ice remaining, are broadly consistent with each other (comparing purple and red lines in Fig. 2). This suggests that it is another shared process, and not the indirect effect of sea ice in the prescribed OHT, which is driving the robust polar-amplified response. We suggest that some of the minor differences between the surface temperature responses in the 1850 annual-mean OHT and $4xCO_2$ annual-mean OHT simulations are caused by the reduction in the amount of poleward OHT in the $4xCO_2$ climate relative to the 1850 climate [cf. Figs. S1b and S1c]. Second, *does including the full seasonal cycle of OHT impact the nature of the polar-amplified response?* Here, the answer is a resounding no. The characteristics of the polar-amplified response in both its magnitude and seasonality are nearly identical in the 1850 annual-mean and seasonal cycle OHT simulations. This is a somewhat unexpected result given how vastly different the individual monthly OHT profiles are to the annual-mean profile (cf. Figs. S1b and S1d). We find that the biggest differences between the surface temperature responses are found in the deep tropics and relate to the position of the intertropical convergence zone, which is not the focus of the current study, rather than the high latitudes (Fig. 2a). Therefore, our results suggest that prescribing an annual-mean OHT may be sufficient for future slab ocean GCM studies investigating polar amplification in ice-free climates.

We now extend our focus from the surface up through the depth of the atmosphere. Figure 4 shows the latitude–height structure of the zonal-mean annual-mean atmospheric temperature response to quadrupled CO_2 for the four experiments. To highlight the differences in the spatial structure, consistent with Fig. 2b, we have normalized by the global-mean annual-mean surface warming. There are two key findings related to the structure of the atmospheric warming per degree of global surface warming. First, the polar amplification that occurs in each of the three OHT experiments is not surface amplified (Figs. 4b–d), as is the case for climates with polar ice caps such as the modern climate (Screen and Simmonds 2010). Instead, the peak of the normalized warming in the polar regions is located in the midtroposphere. The enhanced polar warming response in the midtroposphere is connected to the tropical upper-tropospheric warming along the climatological isentropes. Thus, the structure of the atmospheric warming response provides further evidence to support the hypothesis that surface processes are not responsible for the polar amplification in ice-free climates with OHT and that cloud feedbacks may play an important role. The second takeaway is that the zero OHT experiment features a surface-dominated polar damping (Fig. 4a) that is not present in the OHT experiments. Therefore, the polar amplification in the

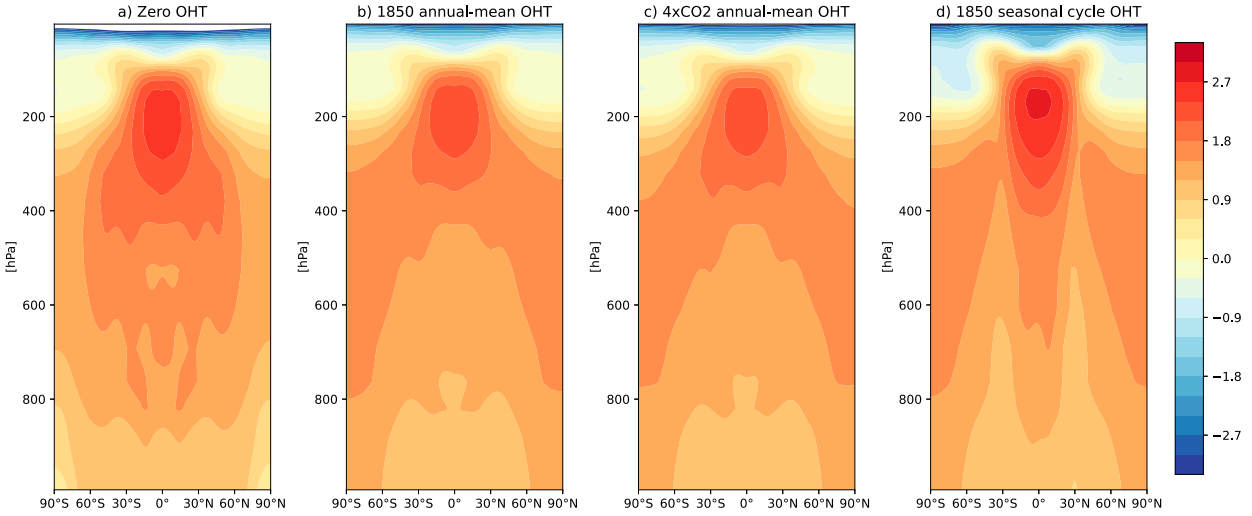

FIG. 4. Latitude–height structure of the zonal-mean annual-mean atmospheric temperature response per degree of global-mean annual-mean surface temperature increase under a quadrupling of CO_2 in the CESM2 aquaplanet simulations prescribed with (a) zero OHT, (b) 1850 annual-mean OHT, (c) 4xCO_2 annual-mean OHT, and (d) 1850 seasonal cycle OHT.

simulations with OHT and the polar damping in the simulations prescribed with zero OHT are driven by processes occurring at different heights in the atmosphere.

It is important to consider whether the influence of the prescribed climatological OHT on the meridional structure of the surface temperature response to a quadrupling of CO_2 is a peculiarity unique to this version of CESM2-CAM6. To investigate the robustness of this result, we have repeated the zero OHT and 1850 annual-mean OHT simulations with CESM1-CAM5. Due to the substantial similarities between the results for the three OHT experiments, it was deemed not necessary to repeat the 4xCO_2 annual-mean OHT and 1850 seasonal cycle OHT experiments. Our main result, namely that polar amplification is strengthened in ice-free climates when a representation of climatological OHT is included, still holds in CESM1-CAM5 (Fig. S2). The CESM1-CAM5 polar amplification factor increases from 1.15 in the zero OHT experiment to 1.26 in the 1850 annual-mean OHT experiment. Further similarities include that the seasonal cycle of polar amplification is more pronounced in the zero OHT simulations than in the OHT experiment (Fig. S2c) and the connection between the tropical upper-tropospheric warming and the polar midtropospheric warming is strengthened in the OHT experiment relative to the zero OHT experiment (Fig. S3). However, one obvious difference between the results presented here for the two different GCMs is that the CESM1-CAM5 zero OHT simulation does not feature the polar damped response that was exhibited in the corresponding CESM2-CAM6 simulation, and instead features a modest amplification at high latitudes. It is therefore difficult to conclude how robust the polar damping simulated by CESM2-CAM6 is, but we do emphasize that the ECHAM6 zero OHT aquaplanet simulations of Shaw and Smith (2022) also feature polar damping with a very similar magnitude (0.75) to the one found in CESM2-CAM6. Taken together, our results from two different GCMs with substantially different cloud parameterizations consistently demonstrate that robust polar amplification *is* possible in climates without sea ice *and* is substantially enhanced by including a representation of OHT, although how this materializes may be somewhat model dependent.

c. *Introducing ocean heat transport enhances polar amplification in CESM2-CAM6 because of shortwave cloud radiative effects*

As the first step in demonstrating the pivotal role clouds play in this story, we will now explore the response of the higher-latitude clouds and CRE to a quadrupling of CO_2 in CESM2-CAM6 and how it differs across our suite of experiments. Decomposing the zonal-mean annual-mean total change in CRE per K of global-mean surface warming (Fig. 5c) into the shortwave contribution (Fig. 5a) and the longwave contribution (Fig. 5b), we find that differences in the shortwave CRE account for the majority of the difference in higher-latitude total CRE response between the OHT and zero OHT experiments and that differences in the longwave CRE are small. This is consistent with the finding from section 3b that the largest seasonal difference in surface temperature response in the OHT and zero OHT experiments is in the summer (Fig. 2c). In the zero OHT experiment, the model simulates a substantial negative shortwave CRE response in the high latitudes to a quadrupling of CO_2 (i.e., a cooling from an increase in the reflection of incoming solar radiation), consistent with the results of Kim et al. (2018). In contrast, the OHT experiments simulate a small negative shortwave CRE response poleward of 70°. Poleward of 60°, the zero OHT experiment simulates a 183 PW K^{-1} cooling of the higher latitudes attributable to the shortwave CRE whereas the same value in the OHT simulations range between a muted cooling of 16 PW K^{-1} to a muted warming of 9 PW K^{-1}.

Thus, the substantial differences in the shortwave CRE response likely explain why the OHT and zero OHT experiments

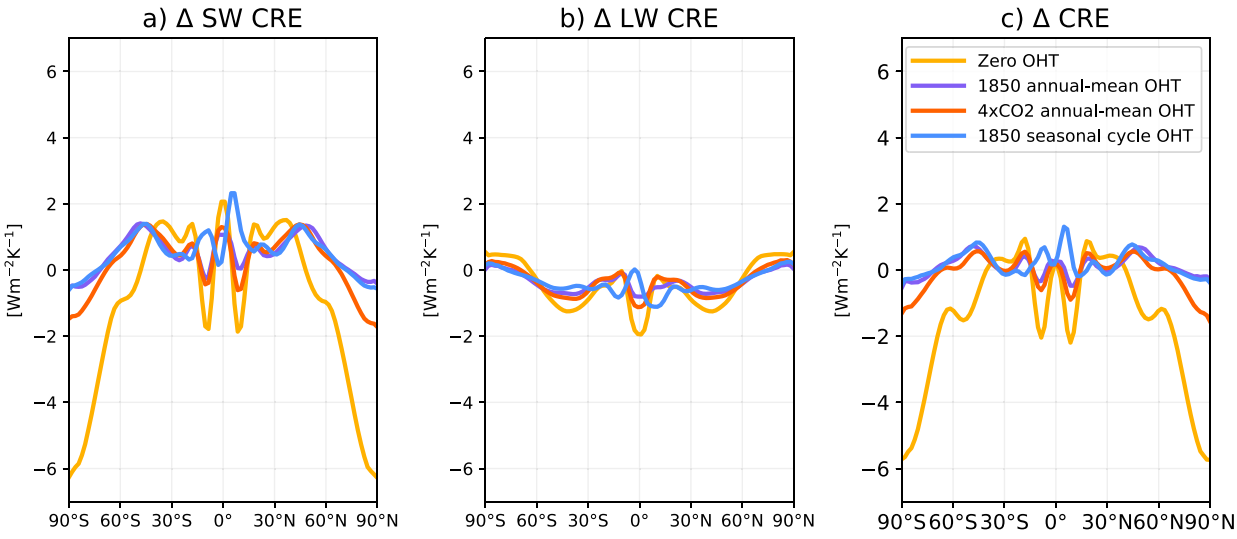

FIG. 5. Zonal-mean annual-mean (a) shortwave CRE, (b) longwave CRE, and (c) total CRE response to a quadrupling of CO_2 in CESM2-CAM6 normalized by the global-mean annual-mean surface warming response for the four experiments.

have such different polar climate responses. The shortwave CRE response can manifest through either a change in the cloud fraction, such that denser cloud coverage is reflecting more incoming solar radiation, or a change in cloud properties, such that a climate with the same cloud fraction but with a higher liquid water content will similarly reflect more incoming solar radiation. We will go on to demonstrate that both mechanisms are important for shaping how climatological OHT influences polar amplification, through the suppression of a large, negative shortwave CRE.

We first examine the cloud fraction response. From this point on, for the purpose of clarity, we will restrict our comparison to the zero OHT and the 1850 annual-mean OHT CESM2-CAM6 experiments. We note that results do not change substantially if we instead compare the zero OHT experiment with either of the other two OHT experiments. Starting from examining the differences in the 1xCO_2 climate (cf. Figs. 6a,b), introducing OHT produces more near-surface clouds at the poles (Fig. 6c), specifically in summer (Fig. S4c; see Southern Hemisphere). Starting from a 1xCO_2 baseline of a larger fraction of near-surface polar clouds, the simulated response to a quadrupling of CO_2 in the 1850 OHT experiment exhibits a substantial decrease in lower- and midtropospheric higher latitude cloud fraction (Fig. 6e). This decrease is most noticeable in winter (Fig. S4e; see Northern Hemisphere) and so will not lead to a substantial increase in absorbed incoming solar radiation. In contrast, the zero OHT experiment features a large increase in near-surface polar clouds (Fig. 6d) in the summer (Fig. S4d), which will result in a substantial damping of polar warming arising from greater reflection of incoming solar radiation and only a muted decrease in lower and midtropospheric cloud fraction. These results are similar to the zero OHT simulations of Kim et al. (2018) [cf. Fig. 3b of Kim et al. (2018) with Fig. 6d herein]. This dependence on the cloud base state is also consistent with the analysis of Vavrus et al. (2009), which found that the CMIP3 intermodel spread in cloud fraction changes over the twenty-first century was connected to the climatological cloud fraction in the twentieth century. Thus, we find that the 1850 annual-mean OHT experiment loses a lot more cloud fraction throughout the higher-latitude atmosphere in response to a quadrupling of CO_2 relative to the zero OHT experiment (Fig. 6f), consistent with a small relative warming contribution rather than a cooling contribution from shortwave CRE.

In addition to differences in the cloud fraction response, there are substantial differences in the climatology and response to a quadrupling of CO_2 in terms of the cloud liquid water content. Again, starting from examining the differences in the 1xCO_2 climate, introducing OHT adds more liquid water to the polar regions and removes liquid water from the tropical troposphere (Fig. 7c), most noticeably in the summer (Fig. S5c; see Southern Hemisphere). The abundant and watery polar clouds in the 1850 annual-mean OHT 1xCO_2 simulation (Fig. 7b) are more efficient at reflecting incoming solar radiation relative to the zero OHT counterpart (Fig. 7a). In the 1850 annual-mean OHT experiment, there is a relatively muted change in liquid water content in response to a quadrupling of CO_2 (Fig. 7e) whereas in the zero OHT experiment under a quadrupling of CO_2 there is a substantial moistening of the lower polar troposphere (Fig. 7d). This increase in the moisture content of clouds is largest in summer (Fig. S5d) and so strongly influences the shortwave CRE. Hence introducing the climatological OHT, relative to the zero OHT experiment, avoids this summer moistening of the lower polar troposphere under a quadrupling of CO_2 and this will result in a less negative shortwave CRE change. We note that changes in cloud ice water content were found to be much less important than liquid water content in CESM2-CAM6 (not shown).

These differences in cloud fraction and liquid water content response paint a consistent picture. Adding climatological

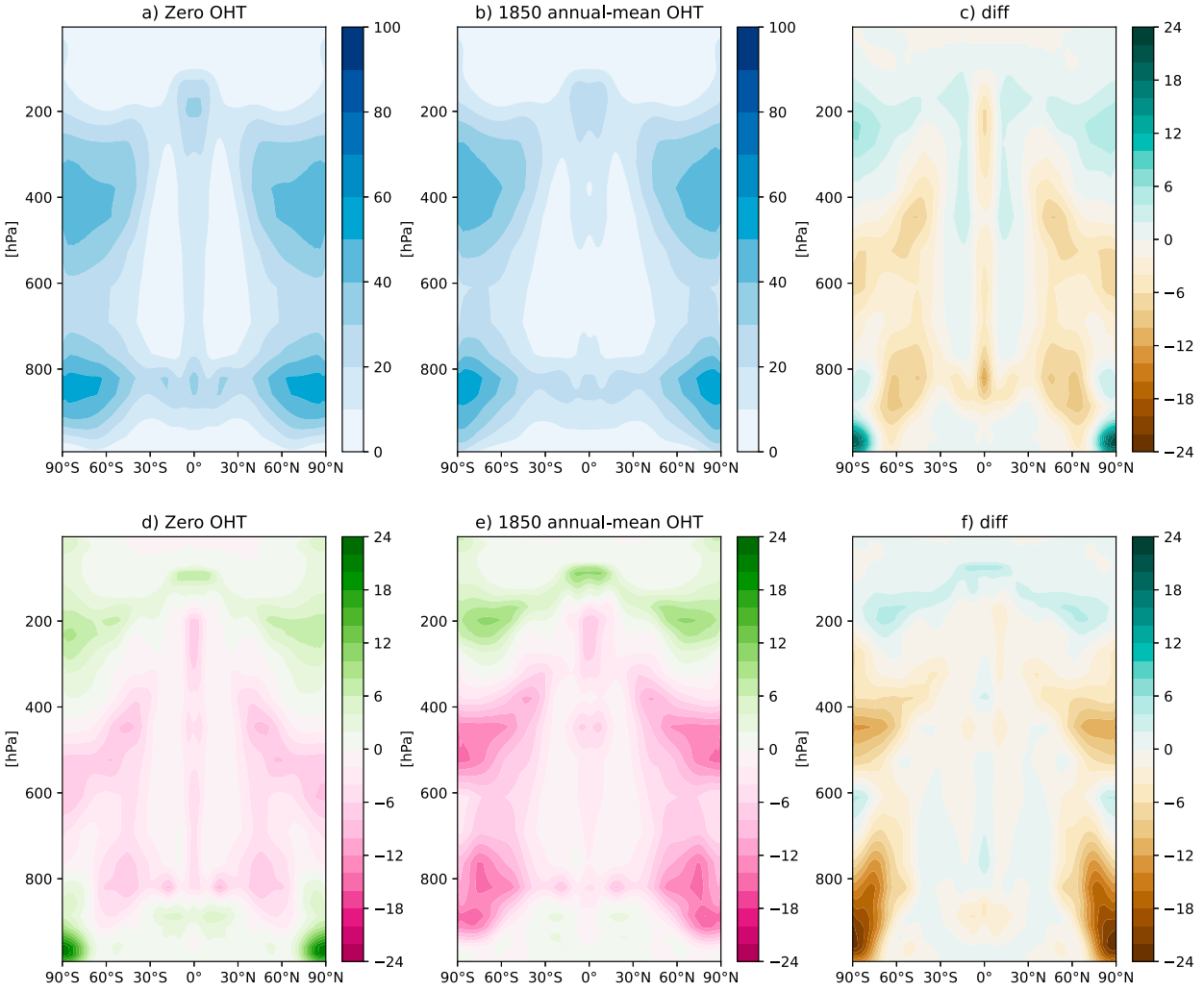

FIG. 6. Zonal-mean annual-mean cloud fraction (%) in 1xCO_2 climate for (a) zero OHT experiment, (b) 1850 annual-mean OHT experiment, and (c) the difference between (b) and (a). (d)–(f) As in (a)–(c), but for the 4xCO_2–1xCO_2 response.

OHT produces a 1xCO_2 climate that has warmer polar regions (Fig. S6), a higher fraction of near-surface polar clouds, and, particularly in the summer, moister lower-tropospheric polar clouds. From this initially moist, cloudy state, there is less cloud gain near the surface (rather, the troposphere is characterized by cloud loss) and less cloud moisture gain relative to the zero OHT experiment as the climate warms in response to a quadrupling of CO_2. In essence, adding climatological OHT inhibits the strong negative high-latitude shortwave CRE change present in the zero OHT experiment. This presents a clear explanation of why polar amplification is stronger in the OHT experiments. These findings are consistent with results from CESM1-CAM5, although ice water content plays a stronger role in that model than CESM2-CAM6 (not shown).

However, while this is a consistent mechanistic explanation, it neither isolates causality nor precludes other factors from being the ultimate cause of why introducing OHT enhances polar amplification in the GCMs. To this end, we turn to cloud locking in CESM2-CAM6 to isolate the role of cloud radiative effects.

d. Cloud locking simulations confirm key role of cloud radiative feedbacks

To quantify the role of CRE in shaping how introducing OHT influences the structure of the meridional surface warming response to increased radiative forcing, we perform cloud locking simulations in CESM2-CAM6. In these simulations, the CRE is prescribed to a desired state, while cloud fraction and microphysics are unconstrained. The question we pose is the following: Given the same change in CRE as the 1850 annual-mean OHT experiment, would we be able to replicate the polar amplification simulated by that experiment but with zero OHT? If so, this demonstrates that introducing the OHT leads to the enhanced polar warming response through modulation by CRE.

Figure 8 compares the shortwave and longwave CRE in the 1xCO_2 and 4xCO_2 climate for the zero OHT, 1850 annual-

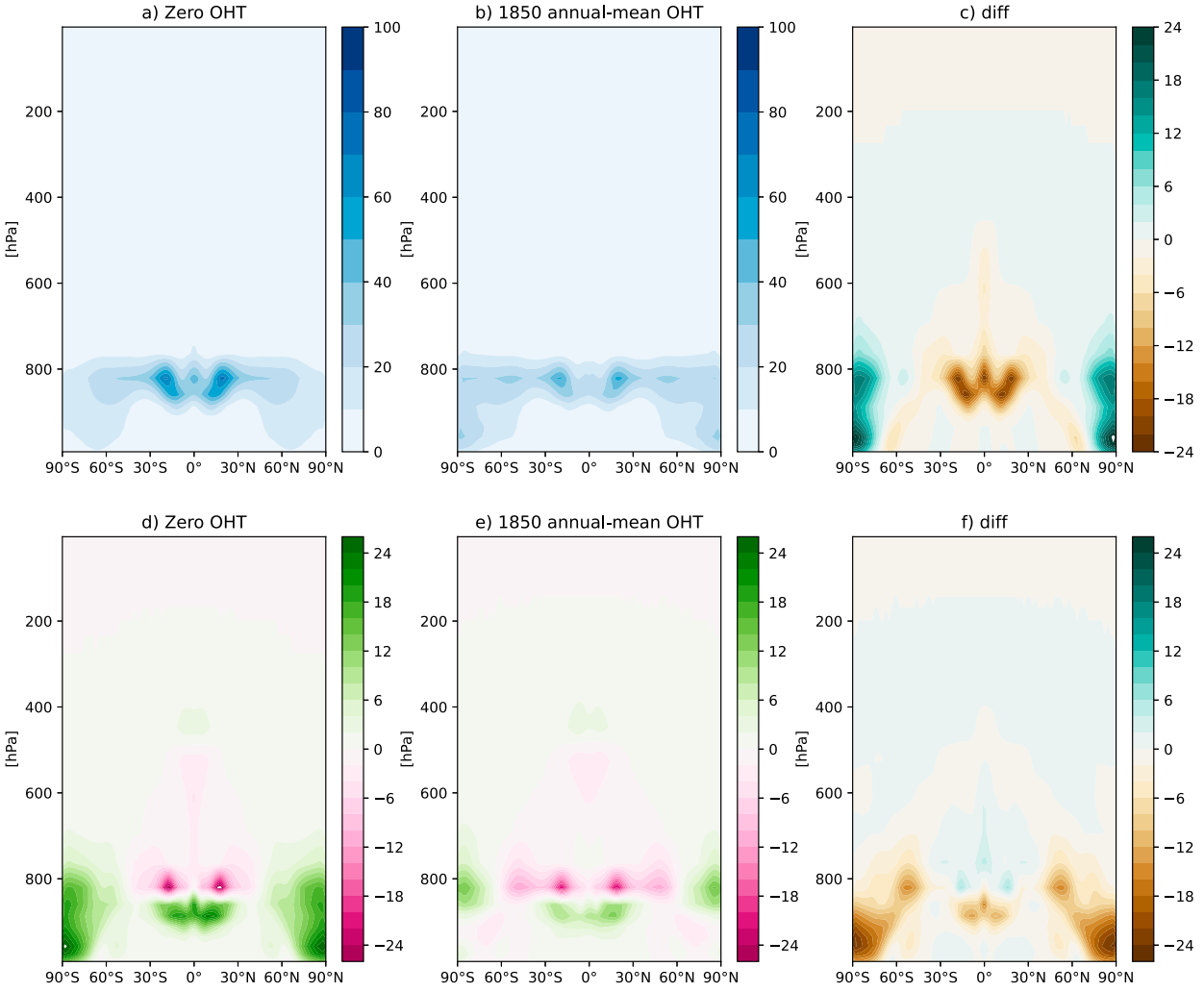

FIG. 7. As in Fig. 6, but for zonal-mean annual-mean liquid water content ($\times 10^{-7}$ kg kg^{-1}).

mean OHT, and zero OHT cloud locking simulations. By design the zero OHT cloud locking simulations closely match the CRE values from the 1850 annual-mean OHT simulation values poleward of 45° and are unconstrained on the equatorward side (cf. Fig. 8, solid purple and dashed pink lines). Note that we do not expect a perfect resemblance because we are locking CRE to 20 years of high-resolution cloud data, rather than the full 100 years. We remind the reader that in the cloud locking simulations we are prescribing the higher-latitude CRE in both the 1xCO_2 and 4xCO_2 climate from the 1850 annual-mean OHT simulations and so are both prescribing the CRE climatology and the CRE response to a quadrupling of CO_2. One noticeable feature of the cloud locked simulations is that in the lower latitudes the CRE departs from both the OHT and zero OHT simulations, with less negative shortwave and less positive longwave CRE in both the 1xCO_2 and 4xCO_2 climate. Locking the higher-latitude CRE in the zero OHT climate results in a warmer tropical climate, with increased surface latent heat flux and increased hydrologic cycle in the deep tropics.

Having demonstrated the efficacy of the cloud locking methodology, we now turn to the main results from the cloud locking simulations. As shown emphatically in Fig. 9, strong polar amplification in the zero OHT simulations is possible if the higher-latitude CREs are prescribed from a simulation with OHT. The annual-mean polar amplification factor increases in the zero OHT experiment from 0.76 before cloud locking to 1.15 after cloud locking, which nearly replicates the 1.19 polar amplification factor from the 1850 annual-mean OHT simulation (Fig. 9b). As a further demonstration of the transformative role of CRE, after cloud locking the seasonal cycle of polar amplification in the zero OHT experiment switches from one dominated by summertime polar damping to one that is polar amplified in every month with near-identical amplitude and phasing to the seasonal cycle from the 1850 annual-mean OHT experiment (Fig. 9c). Using the cloud locking technique, it is not possible to directly tease apart the roles of shortwave and longwave CRE, but we suggest that the shortwave CRE dominates based on our previous discussions on the seasonality of the different responses (Fig. 2c) and because the largest

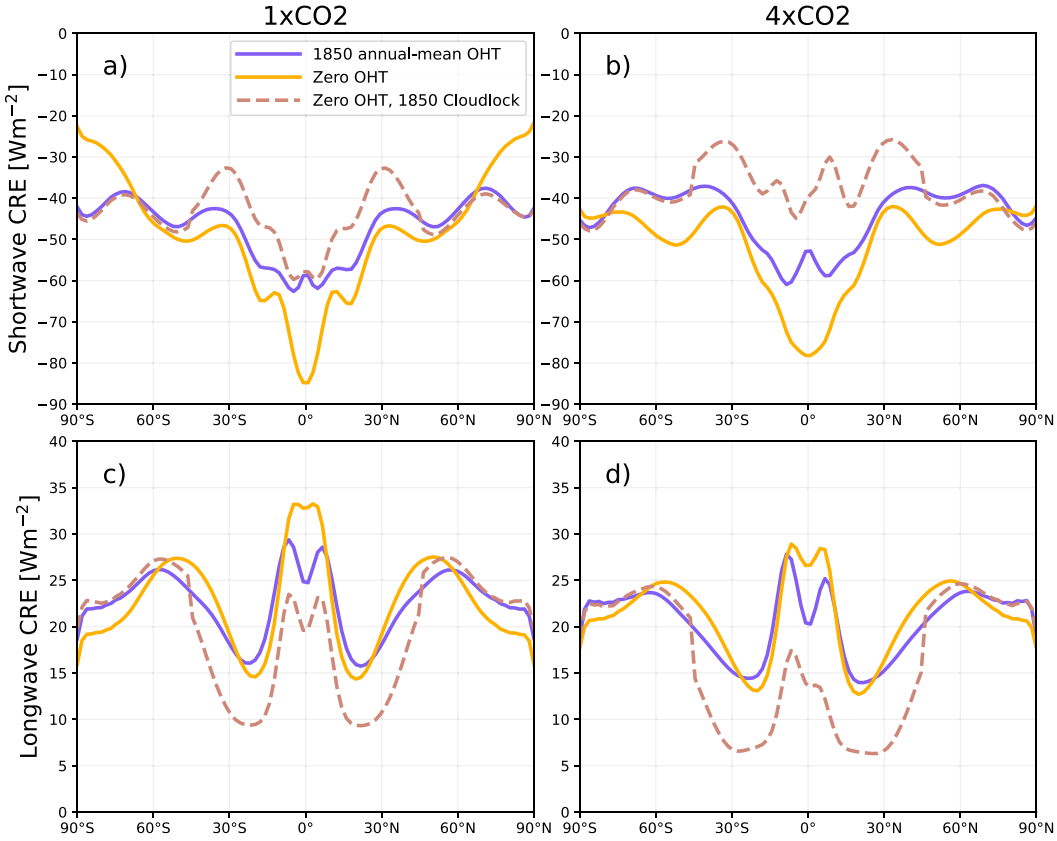

FIG. 8. (top) Zonal-mean annual-mean shortwave and (bottom) longwave CRE in the (left) 1xCO_2 and (right) 4xCO_2 climates in the zero OHT, 1850 annual-mean OHT and zero OHT with higher-latitude cloud locking simulations.

differences in CRE in the unlocked experiments are seen in the shortwave component (Fig. 5a). Last, the extent to which this high-latitude climate response is driven by local processes versus the remote influence of atmospheric heat transport mediated by locking the clouds at the higher latitudes remains to be quantified. We find that the cloud locked simulation transports more heat poleward in response to increased CO_2 than the unlocked simulations (Fig. S7), which potentially suggests a role for interactions between remote factors and higher-latitude cloud feedbacks in facilitating polar amplification in ice-free climates.

Taken together, the results from our targeted cloud locking simulations provide strong causal evidence that the climatological OHT influences polar amplification through setting the climatology of the clouds, consistent with results of Rencurrel and Rose (2018), and predetermining how CRE responds to an increase in CO_2. We are able to reproduce the magnitude and seasonal characteristics of the polar-amplified climate response to increases in radiative forcing solely by altering the CRE. As such, the crux of this polar amplification story, which began with OHT, is revealed to be higher-latitude SW CRE.

4. Summary and discussion

In this study we have investigated the connection between polar amplification, ocean heat transport, and cloud radiative effects in a state-of-the-art GCM, CESM2-CAM6, run in slab ocean aquaplanet configuration. Our main conclusions are as follows: (i) introducing a quasi-realistic climatological OHT enhances the polar-amplified surface temperature response to a quadrupling of CO_2, and in the case of CESM2-CAM6 this reverses a polar damped response found in simulations with no representation of OHT; (ii) the moist diffusive perspective of atmospheric energy transport fails to predict the behavior found in the GCM and in fact predicts the opposite, that introducing a representation of climatological OHT would cause the response to be less polar amplified; and (iii) the mechanism through which the prescribed climatological OHT shapes the meridional structure of the surface warming is through a less negative shortwave cloud feedback as demonstrated by our simulations with cloud locking in the higher latitudes. This decrease in the negative shortwave cloud radiative effect is consistent with ocean–atmosphere heat fluxes preconditioning an avoidance of a large increase in cloud fraction and cloud liquid water in the polar summer months.

The motivation of this study was to explore an inconsistency in past climate modeling studies which disagree on whether ice-free climates exhibit a polar-amplified surface temperature response to an increase in radiative forcing. How can we reconcile the claim that polar amplification is an inherent feature of a moist atmosphere, with or without sea ice,

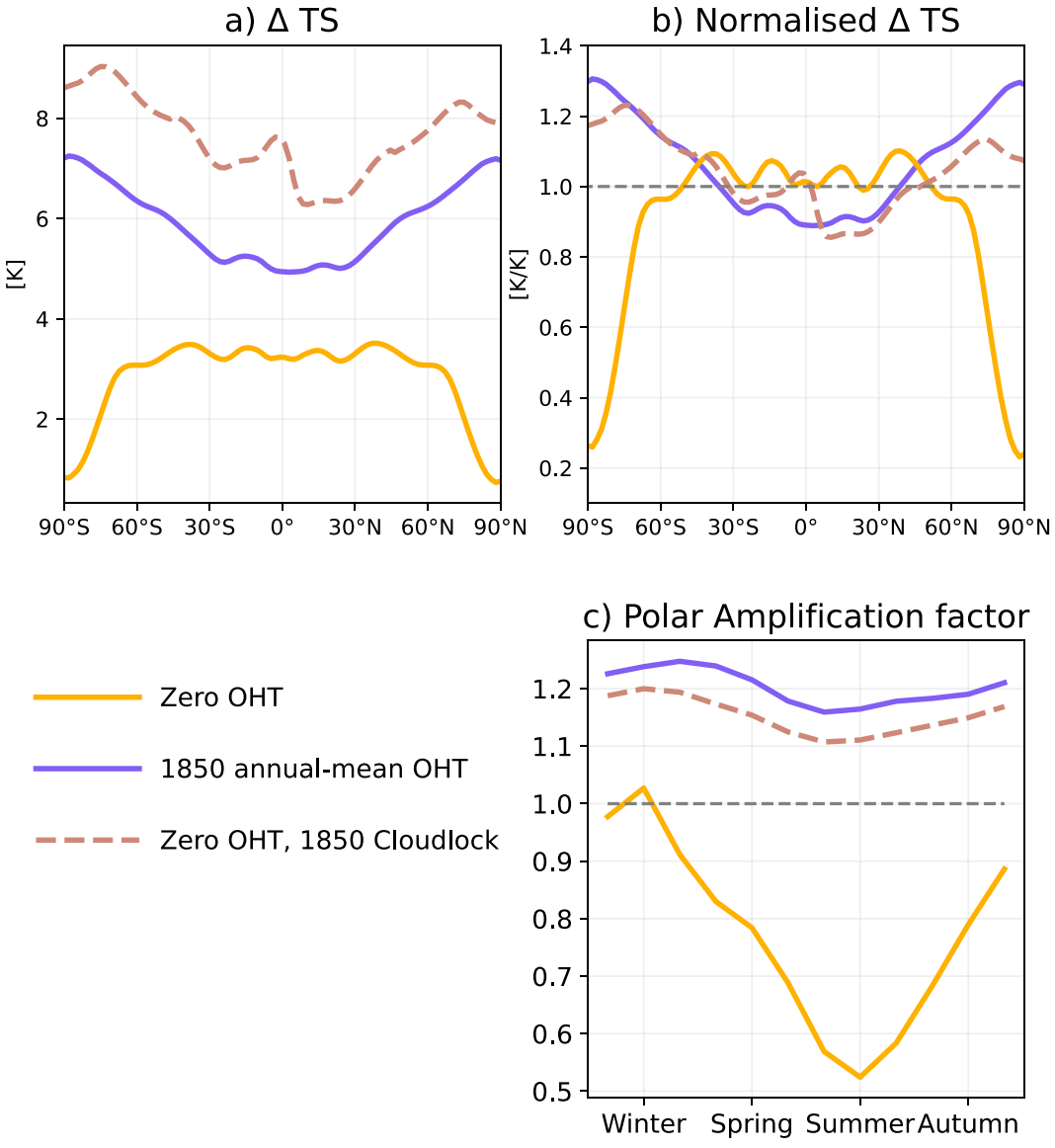

FIG. 9. As in Fig. 2, but for the zero OHT, 1850 annual-mean OHT and zero OHT with cloud locking experiments.

with the claim that sea ice is necessary for polar amplification to occur? Our results based on CESM2-CAM6 slab ocean aquaplanet simulations demonstrate that both claims are somewhat flawed: (i) sea ice is not required for robust polar amplification to occur, although the magnitude of polar amplification is greatly reduced compared to icy climates, and (ii) robust polar amplification is a ubiquitous response of a coupled atmosphere–ocean system. While the first finding is unambiguous, the second finding introduces a nuance into our understanding of polar amplification. We thus reconcile the disparity by presenting a new mechanism for polar amplification that operates in the absence of sea ice and is not controlled by the increase in atmospheric heat transport. It is not impossible to simulate polar amplification in climates with zero OHT, as demonstrated by Rencurrel and Rose (2018) and our simulations with CESM1-CAM5; however, our results suggest that including a quasi-realistic representation of OHT will lead to enhanced polar amplification.

Given that including a representation of climatological OHT in a GCM brings it conceptually closer to the real climate system, we conclude that ice-free climates robustly feature polar enhanced warming, even without the amplifying effect of land (Henry and Vallis 2021), and that neglecting climatological OHT is one idealization too far. There are similarities with this result and the study of Kim et al. (2018) which found that an overly idealized insolation setup led to spurious conclusions about the magnitude of polar amplification in ice-free climates. Using a prescribed zero OHT profile is common in previous slab ocean aquaplanet studies and so our results raise questions about how to interpret some of the

previous findings. We have demonstrated in a single GCM that divergent behavior (both polar amplification and polar damping) can be simulated in response to a quadrupling of CO_2, and that the choice of how to represent OHT can predetermine which response occurs. Stepping back, our study highlights limitations in the conventional interpretation of a climate model hierarchy: here an energy balance model simulated the *opposite* behavior to GCMs because it lacks a representation of clouds, and aquaplanet simulations prescribed with zero OHT simulate the *opposite* behavior to aquaplanet simulations prescribed with a representation of OHT. In each case the idealization would draw you to exactly the wrong conclusion, so it is important to rigorously test simplifying assumptions in a similar manner to our suite of experiments.

What are the implications of our results for far-future climate change? Our aquaplanet simulations have most relevance for understanding Arctic amplification because of the absence of land at the highest latitudes. The main takeaway, especially from the $4xCO_2$ annual-mean OHT simulations, is that Arctic amplification will be a robust feature of the climate system even if most or all of the sea ice cover is lost. The remaining Arctic amplification, however, will be of reduced magnitude and of different seasonality to that of the present-day climate. CMIP5-class models project that nearly all Arctic sea ice cover has melted by the twenty-third century under the high-emissions scenario (Dai et al. 2019). So, according to the results of this study, we would still expect to see Arctic amplification occurring in those simulations past 2200. Despite the main claim about the centrality of sea ice loss for Arctic amplification, the results of Dai et al. (2019) are extremely consistent with our findings: (i) the simulated Arctic warming always exceeds the global-mean warming until 2300 [see Fig. 3d of Dai et al. (2019)]; (ii) the annual-mean Arctic amplification factor is nearly 1.5 for the climate change over the twenty-third century [see Fig. 3c of Dai et al. (2019)], a period that features minimal sea ice loss because the climate is practically ice-free; and (iii) the ice-free Arctic amplification has substantially muted seasonality [again see Fig. 3c of Dai et al. (2019)]. As such, we conclude that our results agree closely with comprehensive climate model simulations featuring ocean dynamics.

Furthermore, this study has implications for how we interpret climate change in past equable climates. Our results provide evidence for why past climates such as the early Eocene had substantially warmer polar regions than the modern climate: the shortwave CRE mechanism identified in this study can be a leading control on the magnitude of polar amplification in ice-free climates. Our results also suggest that the cloud climatology, which influences the meridional structure of the climate response to radiative forcing, depends sensitively on OHT and so constraining OHT in equable climates can improve our understanding of the drivers of past periods of polar amplification. The polar amplification factors we have reported in this study are smaller than has been suggested for the Eocene (Huber and Caballero 2011), Cretaceous (Jenkyns et al. 2004), and Paleogene (Sewall and Sloan 2001) so other processes that are not included in our model, such as the inclusion of land, vegetation feedbacks, changes in orography, and permafrost feedbacks, are likely to be important contributors to polar amplification in past climates (Miller et al. 2010; O'ishi and Abe-Ouchi 2011; Lunt et al. 2012; Henry et al. 2021; Henry and Vallis 2022) in addition to shortwave CRE.

In summation, we have used targeted model experiments with CESM2-CAM6 and CESM1-CAM5 to bring a satisfying resolution to an open question in the literature, concluding that polar amplification is a robust feature of the thermodynamically coupled atmosphere–ocean system. An important avenue of future research will be to investigate the sensitivity of polar cloud feedbacks, and hence polar amplification, to OHT and its changes in climate models beyond the CESM family.

Acknowledgments. This material is based upon work supported by the National Science Foundation (NSF) under award AGS-1753034. MRE is funded by a research fellowship from the Royal Commission for the Exhibition of 1851. Without implying their endorsement, we thank Brian Medeiros and Timothy Merlis for informative discussions. The aquaplanet model used in this study was made available through the Simpler Models Initiative as part of the Community Earth System Model project; this initiative is supported by the National Center for Atmospheric Research (NCAR) under the sponsorship of the NSF. Codes for cloud locking and q-flux calculations were obtained from the NCAR github repositories at https://github.com/NCAR/cesm_cloud_locking and https://github.com/NCAR/simpler_models. We acknowledge use of the lux supercomputer at UC Santa Cruz, funded by NSF MRI grant AST-1828315, and a computing allocation from the CESM Polar Climate Working Group for use of the NCAR Cheyenne supercomputer.

Data availability statement. The processed data and code in the format of a Jupyter Notebook, which are needed to reproduce the results of this study, are available at https://github.com/nfeldl/aquaplanet-qflux.

APPENDIX

Moist Energy Balance Model Setup

We utilize a moist energy balance model (EBM) framework to understand the expected link between the climatological meridional surface climate structure and the nature of the polar-amplified surface temperature response to increased radiative forcing. In this framework atmospheric energy transport is proportional to the meridional gradient of near-surface moist static energy. The EBM used in this study, which includes a seasonally varying representation of insolation, is identical to that used in Feldl and Merlis (2021) except that the thermodynamic sea ice component is removed. In practice, this involves prohibiting sea ice freeze-up by setting the freezing point artificially low. To be clear, this idealized model lacks many of the features found in the CESM aquaplanets, including clouds, a realistic

atmospheric circulation, and a zonally varying climate, but it does offer us fundamental insights into how we might expect polar amplification to depend on the base climate state from the diffusive perspective of moist energy transport.

We conduct pairs of $1xCO_2$ and $4xCO_2$ EBM simulations for the cases of zero OHT and 1850 annual-mean OHT. The zonally averaged q-flux profile is included in the model in the form of an ocean heating term F_b that is added to Eq. (1) of Feldl and Merlis (2021) in the same fashion as in the dry EBM counterpart of Wagner and Eisenman (2015). However, because there is no ice present in our version of the EBM, this term could equivalently be added to the F forcing term of the same equation. Note that the q-flux profile is regridded from the uniform latitude spacing of the CESM aquaplanet input to the uniform area spacing of the EBM. Each simulation is run for 100 years with 1000 timesteps per year with the output averaged over the final year.

Finally, we also include an analytical approximation of the polar amplification factor [Eq. (14) of Merlis and Henry (2018)] based on a truncation of the solution to the moist EBM. The truncated solution depends on the climatological surface temperature, which is needed to determine the change in latent energy transport, and EBM parameters like the longwave feedback parameter and diffusivity. The climate fields are all taken from the $1xCO_2$ control climate and used to predict the polar amplification in the perturbed climate. The truncation to the second Legendre polynomial of the annual-mean surface temperature provides a good estimate of the polar amplification factor as simulated by the moist EBM over a wide range of base climates (Merlis and Henry 2018). The advantage of using this analytical approximation in addition to the moist EBM simulations is that the base climate states from the CESM aquaplanet simulations can be input directly into the truncated solution. This ensures that any differences found between the polar-amplified responses in the CESM aquaplanet simulations and the moist EBM simulations are not attributable to differences in the base state climates.

REFERENCES

Alexeev, V. A., and C. H. Jackson, 2013: Polar amplification: Is atmospheric heat transport important? *Climate Dyn.*, **41**, 533–547, https://doi.org/10.1007/s00382-012-1601-z.

——, P. Langen, and J. Bates, 2005: Polar amplification of surface warming on an aquaplanet in "ghost forcing" experiments without sea ice feedbacks. *Climate Dyn.*, **24**, 655–666, https://doi.org/10.1007/s00382-005-0018-3.

Armour, K. C., N. Siler, A. Donohoe, and G. H. Roe, 2019: Meridional atmospheric heat transport constrained by energetics and mediated by large-scale diffusion. *J. Climate*, **32**, 3655–3680, https://doi.org/10.1175/JCLI-D-18-0563.1.

Bacmeister, J., and Coauthors, 2020: CO_2 increase experiments using the CESM: Relationship to climate sensitivity and comparison of CESM1 to CESM2. *J. Adv. Model. Earth Syst.*, **12**, e2020MS002120, https://doi.org/10.1029/2020MS002120.

Barron, E. J., 1983: A warm, equable Cretaceous: The nature of the problem. *Earth-Sci. Rev.*, **19**, 305–338, https://doi.org/10.1016/0012-8252(83)90001-6.

Beer, E., and I. Eisenman, 2022: Revisiting the role of the water vapor and lapse rate feedbacks in the Arctic amplification of climate change. *J. Climate*, **35**, 2975–2988, https://doi.org/10.1175/JCLI-D-21-0814.1.

——, ——, and T. J. W. Wagner, 2020: Polar amplification due to enhanced heat flux across the halocline. *Geophys. Res. Lett.*, **47**, e2019GL086706, https://doi.org/10.1029/2019GL086706.

Benedict, J. J., B. Medeiros, A. C. Clement, and J. G. Olson, 2020: Investigating the role of cloud-radiation interactions in subseasonal tropical disturbances. *Geophys. Res. Lett.*, **47**, e2019GL086817, https://doi.org/10.1029/2019GL086817.

Cai, M., 2005: Dynamical amplification of polar warming. *Geophys. Res. Lett.*, **32**, L22710, https://doi.org/10.1029/2005GL024481.

——, and J. Lu, 2007: Dynamical greenhouse-plus feedback and polar warming amplification. Part II: Meridional and vertical asymmetries of the global warming. *Climate Dyn.*, **29**, 375–391, https://doi.org/10.1007/s00382-007-0238-9.

Ceppi, P., and D. L. Hartmann, 2016: Clouds and the atmospheric circulation response to warming. *J. Climate*, **29**, 783–799, https://doi.org/10.1175/JCLI-D-15-0394.1.

Chemke, R., 2021: Future changes in the Hadley circulation: The role of ocean heat transport. *Geophys. Res. Lett.*, **48**, e2020GL091372, https://doi.org/10.1029/2020GL091372.

Cronin, T. W., and E. Tziperman, 2015: Low clouds suppress Arctic air formation and amplify high-latitude continental winter warming. *Proc. Natl. Acad. Sci. USA*, **112**, 11 490–11 495, https://doi.org/10.1073/pnas.1510937112.

Dai, A., D. Luo, M. Song, and J. Liu, 2019: Arctic amplification is caused by sea ice loss under increasing CO_2. *Nat. Commun.*, **10**, 121, https://doi.org/10.1038/s41467-018-07954-9.

Danabasoglu, G., and Coauthors, 2020: The Community Earth System Model version 2 (CESM2). *J. Adv. Model. Earth Syst.*, **12**, e2019MS001916, https://doi.org/10.1029/2019MS001916.

Davy, R., L. Chen, and E. Hanna, 2018: Arctic amplification metrics. *Int. J. Climatol.*, **38**, 4384–4394, https://doi.org/10.1002/joc.5675.

Dutta, D., and Coauthors, 2021: A multimodel investigation of atmospheric mechanisms for driving Arctic amplification in warmer climates. *J. Climate*, **34**, 5723–5740, https://doi.org/10.1175/JCLI-D-20-0354.1.

——, S. C. Sherwood, M. Jucker, A. S. Gupta, and K. J. Meissner, 2023: Can polar stratospheric clouds explain Arctic amplification? *J. Climate*, **36**, 2313–2332, https://doi.org/10.1175/JCLI-D-22-0497.1.

England, M., I. Eisenman, N. Lutsko, and T. Wagner, 2021: The recent emergence of Arctic amplification. *Geophys. Res. Lett.*, **48**, e2021GL094086, https://doi.org/10.1029/2021GL094086.

Feldl, N., and G. H. Roe, 2013: The nonlinear and nonlocal nature of climate feedbacks. *J. Climate*, **26**, 8289–8304, https://doi.org/10.1175/JCLI-D-12-00631.1.

——, and T. M. Merlis, 2021: Polar amplification in idealized climates: The role of ice, moisture, and seasons. *Geophys. Res. Lett.*, **48**, e2021GL094130, https://doi.org/10.1029/2021GL094130.

——, S. Bordoni, and T. M. Merlis, 2017: Coupled high-latitude climate feedbacks and their impact on atmospheric heat transport. *J. Climate*, **30**, 189–201, https://doi.org/10.1175/JCLI-D-16-0324.1.

Flannery, B., 1984: Energy balance models incorporating transport of thermal and latent energy. *J. Atmos. Sci.*, **41**, 414–421, https://doi.org/10.1175/1520-0469(1984)041<0414:EBMITO>2.0.CO;2.

Graversen, R. G., and M. Wang, 2009: Polar amplification in a coupled climate model with locked albedo. *Climate Dyn.*, **33**, 629–643, https://doi.org/10.1007/s00382-009-0535-6.

——, and P. L. Langen, 2019: On the role of the atmospheric energy transport in 2 × CO_2-induced polar amplification in CESM1. *J. Climate*, **32**, 3941–3956, https://doi.org/10.1175/JCLI-D-18-0546.1.

——, ——, and T. Mauritsen, 2014: Polar amplification in CCSM4: Contributions from the lapse rate and surface albedo feedbacks. *J. Climate*, **27**, 4433–4450, https://doi.org/10.1175/JCLI-D-13-00551.1.

Grise, K., B. Medeiros, J. J. Benedict, and J. G. Olson, 2019: Investigating the influence of cloud radiative effects on the extratropical storm tracks. *Geophys. Res. Lett.*, **46**, 7700–7707, https://doi.org/10.1029/2019GL083542.

Hahn, L. C., K. C. Armour, M. D. Zelinka, C. M. Bitz, and A. Donohoe, 2021: Contributions to polar amplification in CMIP5 and CMIP6 models. *Front. Earth Sci.*, **9**, 710036, https://doi.org/10.3389/feart.2021.710036.

——, ——, D. S. Battisti, I. Eisenman, and C. M. Bitz, 2022: Seasonality in Arctic warming driven by sea ice effective heat capacity. *J. Climate*, **35**, 1629–1642, https://doi.org/10.1175/JCLI-D-21-0626.1.

Hall, A., 2004: The role of surface albedo feedback in climate. *J. Climate*, **17**, 1550–1568, https://doi.org/10.1175/1520-0442(2004)017<1550:TROSAF>2.0.CO;2.

Henry, M., and G. Vallis, 2021: Reduced high-latitude land seasonality in climates with very high carbon dioxide. *J. Climate*, **34**, 7325–7336, https://doi.org/10.1175/JCLI-D-21-0131.1.

——, and ——, 2022: Variations on a pathway to an early Eocene climate. *Paleoceanogr. Paleoclimatol.*, **37**, e2021PA004375, https://doi.org/10.1029/2021PA004375.

——, T. M. Merlis, N. J. Lutsko, and B. E. J. Rose, 2021: Decomposing the drivers of polar amplification with a single column model. *J. Climate*, **34**, 2355–2365, https://doi.org/10.1175/JCLI-D-20-0178.1.

Holland, M. M., and C. M. Bitz, 2003: Polar amplification of climate change in coupled models. *Climate Dyn.*, **21**, 221–232, https://doi.org/10.1007/s00382-003-0332-6.

Huber, M., and R. Caballero, 2011: The early Eocene equable climate problem revisited. *Climate Past*, **7**, 603–633, https://doi.org/10.5194/cp-7-603-2011.

Hwang, Y.-T., D. M. W. Frierson, and J. E. Kay, 2011: Coupling between Arctic feedbacks and changes in poleward energy transport. *Geophys. Res. Lett.*, **38**, L17704, https://doi.org/10.1029/2011GL048546.

Jenkyns, H., A. Forster, S. Schouten, and J. Damste, 2004: High temperatures in the late Cretaceous Arctic Ocean. *Nature*, **432**, 888–892, https://doi.org/10.1038/nature03143.

Kay, J., M. Holland, C. Bitz, E. Blanchard-Wrigglesworth, A. Gettelman, A. Conley, and D. Bailey, 2012: The influence of local feedbacks and northward heat transport on the equilibrium Arctic climate response to increased greenhouse gas forcing. *J. Climate*, **25**, 5433–5450, https://doi.org/10.1175/JCLI-D-11-00622.1.

——, T. L'Ecuyer, H. Chepfer, N. Loeb, A. Morrison, and G. Cesana, 2016: Recent advances in Arctic cloud and climate research. *Curr. Climate Change Rep.*, **2**, 159–169, https://doi.org/10.1007/s40641-016-0051-9.

Kim, D., S. M. Kang, Y. Shin, and N. Feldl, 2018: Sensitivity of polar amplification to varying insolation conditions. *J. Climate*, **31**, 4933–4947, https://doi.org/10.1175/JCLI-D-17-0627.1.

Kumar, A., and Coauthors, 2010: Contribution of sea ice loss to Arctic amplification. *Geophys. Res. Lett.*, **37**, L21701, https://doi.org/10.1029/2010GL045022.

Langen, P. L., and V. A. Alexeev, 2007: Polar amplification as a preferred response in an idealized aquaplanet GCM. *Climate Dyn.*, **29**, 305–317, https://doi.org/10.1007/s00382-006-0221-x.

——, R. G. Graversen, and T. Mauritsen, 2012: Separation of contributions from radiative feedbacks to polar amplification on an aquaplanet. *J. Climate*, **25**, 3010–3024, https://doi.org/10.1175/JCLI-D-11-00246.1.

Lunt, D. J., A. M. Haywood, G. A. Schmidt, U. Salzmann, P. J. Valdes, H. J. Dowsett, and C. A. Loptson, 2012: On the causes of mid-Pliocene warmth and polar amplification. *Earth Planet. Sci. Lett.*, **321–322**, 128–138, https://doi.org/10.1016/j.epsl.2011.12.042.

Manabe, S., and R. T. Wetherald, 1975: The effects of doubling the CO_2 concentration on the climate of a general circulation model. *J. Atmos. Sci.*, **32**, 3–15, https://doi.org/10.1175/1520-0469(1975)032<0003:TEODTC>2.0.CO;2.

McIlhattan, E. A., J. E. Kay, and T. S. L'Ecuyer, 2020: Arctic clouds and precipitation in the Community Earth System Model version 2. *J. Geophys. Res. Atmos.*, **125**, e2020JC032521, https://doi.org/10.1029/2020JD032521.

Medeiros, B., D. L. Williamson, and J. G. Olson, 2016: Reference aquaplanet climate in the Community Atmosphere Model, version 5. *J. Adv. Model. Earth Syst.*, **8**, 406–424, https://doi.org/10.1002/2015MS000593.

——, A. C. Clement, J. J. Benedict, and B. Zhang, 2021: Investigating the impact of cloud-radiative feedbacks on tropical precipitation extremes. *npj Climate Atmos. Sci.*, **4**, 18, https://doi.org/10.1038/s41612-021-00174-x.

Merlis, T., and M. Henry, 2018: Simple estimates of polar amplification in moist diffusive energy balance models. *J. Climate*, **31**, 5811–5824, https://doi.org/10.1175/JCLI-D-17-0578.1.

Middlemas, E. A., J. E. Kay, B. M. Medeiros, and E. A. Maroon, 2020: Quantifying the influence of cloud radiative feedbacks on Arctic surface warming using cloud locking in an Earth System Model. *Geophys. Res. Lett.*, **47**, e2020GL089207, https://doi.org/10.1029/2020GL089207.

Miller, G. H., R. B. Alley, J. Brigham-Grette, J. J. Fitzpatrick, L. Polyak, M. C. Serreze, and J. W. C. White, 2010: Arctic amplification: Can the past constrain the future? *Quat. Sci. Rev.*, **29**, 1779–1790, https://doi.org/10.1016/j.quascirev.2010.02.008.

O'ishi, R., and A. Abe-Ouchi, 2011: Polar amplification in the mid-Holocene derived from dynamical vegetation change with a GCM. *Geophys. Res. Lett.*, **38**, L14702, https://doi.org/10.1029/2011GL048001.

Park, K., S. Kang, D. Kim, M. F. Stuecker, and F.-F. Jin, 2018: Contrasting local and remote impacts of surface heating on polar warming and amplification. *J. Climate*, **31**, 3155–3166, https://doi.org/10.1175/JCLI-D-17-0600.1.

Pithan, F., and T. Mauritsen, 2014: Arctic amplification dominated by temperature feedbacks in contemporary climate models. *Nat. Geosci.*, **7**, 181–184, https://doi.org/10.1038/ngeo2071.

Polvani, L. M., A. C. Clement, J. J. Benedict, and I. R. Simpson, 2017: When less is more: Opening the door to simpler climate models. *Eos*, **98**, https://doi.org/10.1029/2017EO079417.

Previdi, M., K. L. Smith, and L. M. Polvani, 2021: Arctic amplification of climate change: A review of underlying mechanisms. *Environ. Res. Lett.*, **16**, 093003, https://doi.org/10.1088/1748-9326/ac1c29.

Rädel, G., T. Mauritsen, B. Stevens, D. Dommenget, D. Matei, K. Bellomo, and A. Clement, 2016: Amplification of El Niño

by cloud longwave coupling to atmospheric circulation. *Nat. Geosci.*, **9**, 106–110, https://doi.org/10.1038/ngeo2630.

Rencurrel, M. C., and B. E. J. Rose, 2018: Exploring the climatic response to wide variations in ocean heat transport on an aquaplanet. *J. Climate*, **31**, 6299–6318, https://doi.org/10.1175/JCLI-D-17-0856.1.

Rodgers, K. B., G. Lohmann, S. Lorenz, R. Schneider, and G. M. Henderson, 2003: A tropical mechanism for Northern Hemisphere deglaciation. *Geochem. Geophys. Geosyst.*, **4**, 1046, https://doi.org/10.1029/2003GC000508.

Roe, G. H., N. Feldl, K. C. Armour, Y.-T. Hwang, and D. M. W. Frierson, 2015: The remote impacts of climate feedbacks on regional climate predictability. *Nat. Geosci.*, **8**, 135–139, https://doi.org/10.1038/ngeo2346.

Rose, B. E. J., and D. Ferreira, 2013: Ocean heat transport and water vapor greenhouse in a warm equable climate: A new look at the low gradient paradox. *J. Climate*, **26**, 2117–2136, https://doi.org/10.1175/JCLI-D-11-00547.1.

——, K. C. Armour, D. S. Battisti, N. Feldl, and D. D. B. Koll, 2014: The dependence of transient climate sensitivity and radiative feedbacks on the spatial pattern of ocean heat uptake. *Geophys. Res. Lett.*, **41**, 1071–1078, https://doi.org/10.1002/2013GL058955.

Russotto, R., and M. Biasutti, 2020: Polar amplification as an inherent response of a circulating atmosphere: Results from the TRACMIP aquaplanets. *Geophys. Res. Lett.*, **47**, e2019GL086771, https://doi.org/10.1029/2019GL086771.

Screen, J. A., and I. Simmonds, 2010: The central role of diminishing sea ice in recent Arctic temperature amplification. *Nature*, **464**, 1334–1337, https://doi.org/10.1038/nature09051.

Sewall, J. O., and L. C. Sloan, 2001: Equable paleogene climates: The result of a stable, positive Arctic Oscillation? *Geophys. Res. Lett.*, **28**, 3693–3695, https://doi.org/10.1029/2001GL013776.

Shaw, T. A., and Z. Smith, 2022: The midlatitude response to polar sea ice loss: Idealized slab-ocean aquaplanet experiments with thermodynamic sea ice. *J. Climate*, **35**, 2633–2649, https://doi.org/10.1175/JCLI-D-21-0508.1.

Simpson, I. R., and Coauthors, 2020: An evaluation of the large-scale atmospheric circulation and its variability in CESM2 and other CMIP models. *J. Geophys. Res. Atmos.*, **125**, e2020JD032835, https://doi.org/10.1029/2020JD032835.

Singh, H., N. Feldl, J. E. Kay, and A. L. Morrison, 2022: Climate sensitivity is sensitive to changes in ocean heat transport. *J. Climate*, **35**, 2653–2674, https://doi.org/10.1175/JCLI-D-21-0674.1.

Södergren, A. H., A. J. McDonald, and G. E. Bodeker, 2018: An energy balance model exploration of the impacts of interactions between surface albedo, cloud cover and water vapor on polar amplification. *Climate Dyn.*, **51**, 1639–1658, https://doi.org/10.1007/s00382-017-3974-5.

Tan, I., and T. Storelvmo, 2019: Evidence of strong contributions from mixed-phase clouds to Arctic climate change. *Geophys. Res. Lett.*, **46**, 2894–2902, https://doi.org/10.1029/2018GL081871.

——, D. Barahona, and Q. Coopman, 2022: Potential link between ice nucleation and climate model spread in Arctic amplification. *Geophys. Res. Lett.*, **49**, e2021GL097373, https://doi.org/10.1029/2021GL097373.

Taylor, P. C., M. Cai, A. Hu, J. Meehl, W. Washington, and G. J. Zhang, 2013: A decomposition of feedback contributions to polar warming amplification. *J. Climate*, **26**, 7023–7043, https://doi.org/10.1175/JCLI-D-12-00696.1.

Vavrus, S., D. Waliser, A. Schweiger, and J. Francis, 2009: Simulations of 20th and 21st century Arctic cloud amount in the global climate models assessed in the IPCC AR4. *Climate Dyn.*, **33**, 1099–1115, https://doi.org/10.1007/s00382-008-0475-6.

——, U. S. Bhatt, and V. A. Alexeev, 2011a: Factors influencing simulated changes in future Arctic cloudiness. *J. Climate*, **24**, 4817–4830, https://doi.org/10.1175/2011JCLI4029.1.

——, M. Holland, and D. Bailey, 2011b: Changes in Arctic clouds during intervals of rapid sea ice loss. *Climate Dyn.*, **36**, 1475–1489, https://doi.org/10.1007/s00382-010-0816-0.

Wagner, T. J. W., and I. Eisenman, 2015: How climate model complexity influences sea ice stability. *J. Climate*, **28**, 3998–4014, https://doi.org/10.1175/JCLI-D-14-00654.1.

Zhu, J., C. J. Poulsen, and J. E. Tierney, 2019: Simulation of Eocene extreme warmth and high climate sensitivity through cloud feedbacks. *Sci. Adv.*, **5**, eeax1874, https://doi.org/10.1126/sciadv.aax1874.

——, and Coauthors, 2022: LGM paleoclimate constraints inform cloud parameterizations and equilibrium climate sensitivity in CESM2. *J. Adv. Model. Earth Syst.*, **14**, e2021MS002776, https://doi.org/10.1029/2021MS002776.